WATER SURFACE PROFILES

USING FESWMS-2DH

MODEL

By

DIMITRI G. STRONGYLIS

Bachelor of Science

The University of Oklahoma

Norman, Oklahoma

1988

Submitted to the Faculty of the
Graduate College of the
Oklahoma State University
in partial fulfillment of
the requirments for
the Degree of
MASTER OF SCIENCE
July, 1992

WATER SURFACE PROFILES

USING FESWMS-2DH

MODEL

Thesis Approved:

Thesis Advisor

Dean of the Graduate College

PREFACE

In the study of hydraulic problems very few computerized approaches are available. All of these approaches use 18th century methodology and they are solving the problem in one dimension by making considerable simplifications as to the uniformity of the physical conditions from one point of study to another.

FESWMS-2DH makes no simplifications at all and considers the dynamics of flow in both the two horizontal dimensions and the vertical dimension. FESWMS-2DH is a very flexible model and can study very intricate flow conditions. The use of FESWMS-2DH is encouraged in every case in which multidimensional flow is evident or suspected.

I wish to express my sincere gratitude to the individuals who assisted me in this project and during my coursework at Oklahoma State University. In particular I wish to thank my major advisor Dr. A.K. Tyagi, for his intelligent guidance, inspiration, and invaluable assistance. I am also grateful to the other committee members, Dr. Mast and Dr. Carter for their advisement during the course of this work.

Special thanks are due to the Oklahoma Department of Transportation Hydraulic Branch which provided the information needed for this study and the utilization of the

computer hardware and software.

The help of the Hydraulic Branch Engineering manager Gary Brown and Engineers Zia Siavashpour and Fred Rasolkhani is sincerely appreciated.

Special thanks are also in order to Robert Spalik for doing the typesetting on this manuscript.

TABLE OF CONTENTS

LIST OF TABLES

LIST OF ACRONYMS AND SYMBOLS

1. FESWMS-2DH - Finite Element Surface-Water Modeling System: 2 Dimension Horizontal
2. HY-4 - A computer program for Hydraulics of Bridge Waterways (BPR Program HY-4-69)
3. HEC-2 - Hydrologic Engineering Center Water Surface Profiles
4. Q_5 - Runoff produced at the 5 year event
5. Q_{10} - Runoff produced at the 10 year event
6. Q_{25} - Runoff produced at the 25 year event
7. Q_{50} - Runoff produced at the 50 year event
8. SCS - Soil Conservation Service
9. USGS - United States Geological Survey
10. Q_{100} - Runoff produced at the 100 year event
11. V_5 - Velocity resulting from the 5 year event
12. V_{10} - Velocity resulting from the 10 year event
13. V_{25} - Velocity resulting from the 25 year event
14. V_{50} - Velocity resulting from the 50 year event
15. V_{100} - Velocity resulting from the 100 year event
16. WSEL - Water Surface Elevation
17. WSPRO - Water Surface Profiles

LIST OF FIGURES

CHAPTER I

INTRODUCTION

STATEMENT OF THE PROBLEM

Location

The Cimarron River originates in New Mexico. The river initially enters and exits the State of Oklahoma at Cimarron County, then it reenters the state at Beaver County and exits at Harper County. Then the river enters the State of Oklahoma for the third time and forms part of the eastern portion of the Harper County line. The river then flows in a southeasterly direction to its termination at the Keystone Reservoir. The drainage area contributing runoff to the river up to the crossing with Interstate-35, north of Guthrie is 17,505 square miles of which 4,296 square miles are non-contributing. (They are controlled by SCS water dentntion structures). The channel is 700 - 2000 feet wide and meandering with high banks. The valley varies in width from (0.8 - 1.2) miles and it is about one mile wide at the vicinity of the Interstate-35 crossing (Pictorial History, Appendix A). History indicates that the meander leg just upstream from the Interstate-35 crossing is progressing downstream with a tendency for the main channel to move north in the floodplain. Currently the main channel is at

the southern edge of the floodplain.

Flood Events

The most severe floods on record occurred in May of 1957 and in October of 1986. No discharge is available for the 1957 flood, but the water reached an elevation of 899.0 feet. The flood of 1986 had a peak discharge of 156,000 cubic feet per second, (Q_{52}) with a corresponding water surface elevation of 898.0

Crossing Characteristics

The river exhibits a degree of meandering and the Interstate-35 crossing appears to be forcing the flow into a rather sharp turn in order to go under the main structure. The main structure is 800 feet long and is located at the southern edge of the river valley. The overflow structure is located at the northern edge with a length of 1,360 feet. The overflow structure has a flowline elevation of 16.5 feet higher than the main structure (887.0 versus 870.5), respectively.

Scope of the Investigation

The scope of this investigation is to establish water surface elevations and velocities at several points of the Interstate-35 and Cimarron River crossing for Q-5, Q-10, Q-25, Q-50 and Q-100 events, and compare with the existing results of WSPRO and HY-4.

This study is intended for use as a base for future

evaluation of possible solutions (jetties, spur dikes, etc.) in an effect to control the river's natural tendency to meander.

This study will also provide information (velocities and water surface elevations) needed to accurately evaluate potential problems at the main and overflow structures (such as scour).

CHAPTER II

REVIEW OF LITERATURE

Background

The finite element method is a numerical procedure for solving the differential equations encountered in problems of physics and engineering. The development of the method has been encouraged primarily by the continued advancement of high speed digital computers which provide a means of performing rapidly the many calculations involved in the method.

Fundamental Concepts

The fundamental concept of the finite element method is that any smooth quantity can be approximated by a discrete model composed of a set of piecewise-smooth functions which are defined over a finite number of subdomains called elements. The piecewise-smooth functions are called interpolation, shape, trial, or basis functions. These functions are described in terms of the values of the smooth quantity of a finite number of points in its domain, and are typically polynomials of the third or fifth degree. The points at which the quantity is defined are called nodes and are usually located along the element boundaries where

adjacent elements are considered to be connected, although some nodes may be positioned in the element interiors.

The nodal values of the quantity being modeled along with the selected interpolation functions, completely describe the variation of the quantity within each element. For the infinite element solution of the problem the nodal values become the unknowns. The behavior of the solution throughout the assemplage of elements is described by the interpolation functions once the unknown nodal quantities are found.

Clearly the interpolation functions cannot be selected arbitrarily; they should be able to approximate the true time distribution of the field variable as closely as possible. In addition, at the element boundaries, the field variables and any of its partial derivatives up to one order less than the highest order derivative of the equation being solved must be continuous. This is known as the compatibility requirement. Elements whose interpolation function satisfy this requirement, are known as compatible and conforming elements. Another condition that must be satisfied is that as the element size shrinks, the zero values of the field variable and all of its partial derivatives up to the highest order appearing in the equation being solved must be constant over an infinitesimal part of the solution domain. This is known as the completeness requirement.

Once the finite-element model has been established (that is, the elements and their interpolation functions

have been chosen), the derivation of the element equations may be achieved by direct methods, variational methods, or weighted residual methods.

Direct methods for deriving finite element equations are based on direct physical reasoning but can be applied only for relatively simple problems and element shapes. However, the finite-element equations that are found by the direct physical reasoning can also be achieved by minimizing an energy function (Becker and others 1981, p. 60), with respect to the nodal variables. Thus a general method for formulating the finite element equations is obtained by applying variational principals governing the particular problem of interest.

The variational approach to deriving element equations is the most widely used and it is the most convenient when a classical variational statement exists for a particular problem. However, many practical problems are encountered for which classical variational principles are unknown. In these cases, more generalized procedures must be used to derive the element equations.

Weighted residual methods are general techniques for obtaining approximate solutions to linear and non-linear partial differential equations and include collation, least squares, and Galerkin methods. In all these, the unknown solution is approximated by a set of interpolation functions containing adjustable constants or functions. The chosen constants or functions define the type of weighted residual method and attempt to provide the "best" approximation of

the exact solution. Although the methods of weighted residuals offer a more general means of formulating the element equations, they are not directly related to the finite-element method. The technique most often used to derive finite-element equations is known as Galerkin's method. In this method, the same as the interpolation functions of the trial solution. Thus Galerkin's method requires that

$$\int_R N_i(L\hat{u} - f)\, dR = 0, \text{ for } i = 1, 2, \ldots, m . \qquad (2\text{-}2)$$

where N_i is the assumed interpolation function, L is a differential operator, u is the unknown nodal variable, f is a known function and R is the domain. Also the differential equation for a problem can be written as

$$Lu - f = 0 \qquad (2\text{-}2)$$

The left hand side of eq. 2-1 can be written as the sum of expressions governing the behavior of eq. 2-2 on individual elements. The variable u can be approximated with respect to the element as

$$\hat{u}^{(e)} = \sum_{i=1}^{n} N_i^{(e)}\, u_i^{(e)} \qquad (2\text{-}3)$$

where the subscript (e) denotes the restriction of the relevant variable of function to the element and n is the number of unknown nodal variables assigned to the element. Then the left-hand side of equation 2-1 can be written as the sum of expressions of the form

$$\int_{R^{(e)}} N_i^{(e)} (L\hat{u}^{(e)} - f^{(e)})\, dR^{(e)}; \text{ for } i = 1, 2, \ldots, n, \quad (2\text{-}4)$$

A set of such expressions can be developed for an element of the system and then combined. This assembly of the element, or local, expressions results in a set of global algebraic equations, which must be solved simultaneously. In many cases, it is possible to reduce the order of derivatives contained in the governing differential equation by applying integration of the finite-element equation. Hence, the interpolation functions will be required to satisfy a less stringent compatibility condition. Not only will the choice of approximating functions be less restricted, but the surface or line integrals that arise from integration by parts provide a convenient means of applying certain boundary conditions which are called 'natural boundary conditions'. These boundary integral terms are then usually moved to the right-hand side of the system of the finite element equations. Although these boundary terms will appear in the equations of every element of the system, they need only to be evaluated on the boundary elements since all integral contributions will cancel. Essential boundary conditions can be applied to the combined system of equations once the assembly process is complete. 'Essential boundary conditions' are those that the nodal values are required to satisfy directly. They are usually introduced by eliminating the finite-element equations that govern the relevant nodal variables.

The basic idea of the finite-element method is that a solution domain of arbitrary shape can be discretized by assumptions of elements in such a way that a sequence of approximate solutions defined on successively more defined discretizations will converge to the exact solution of the governing differential equations. In many cases, these elements are geometrically fairly simple. Common two dimensional elements are shown in fig II-1. The three node triangle is the simplest element that can be used to define the linear variation of a quantity in two dimensions. Because of its simplicity and its ability to model domains at nearly any shape, it is the most frequently used two-dimensional finite-element. The four-node quadrilateral is another commonly used linear two-dimensional element and may be formed directly or by the combination of two or four linear triangles. Elements with additional nodes are used to define higher order approximating functions. For example a six-node triangle can be used to model the quadratic variation of a field variable along with the nine node quadrilateral.

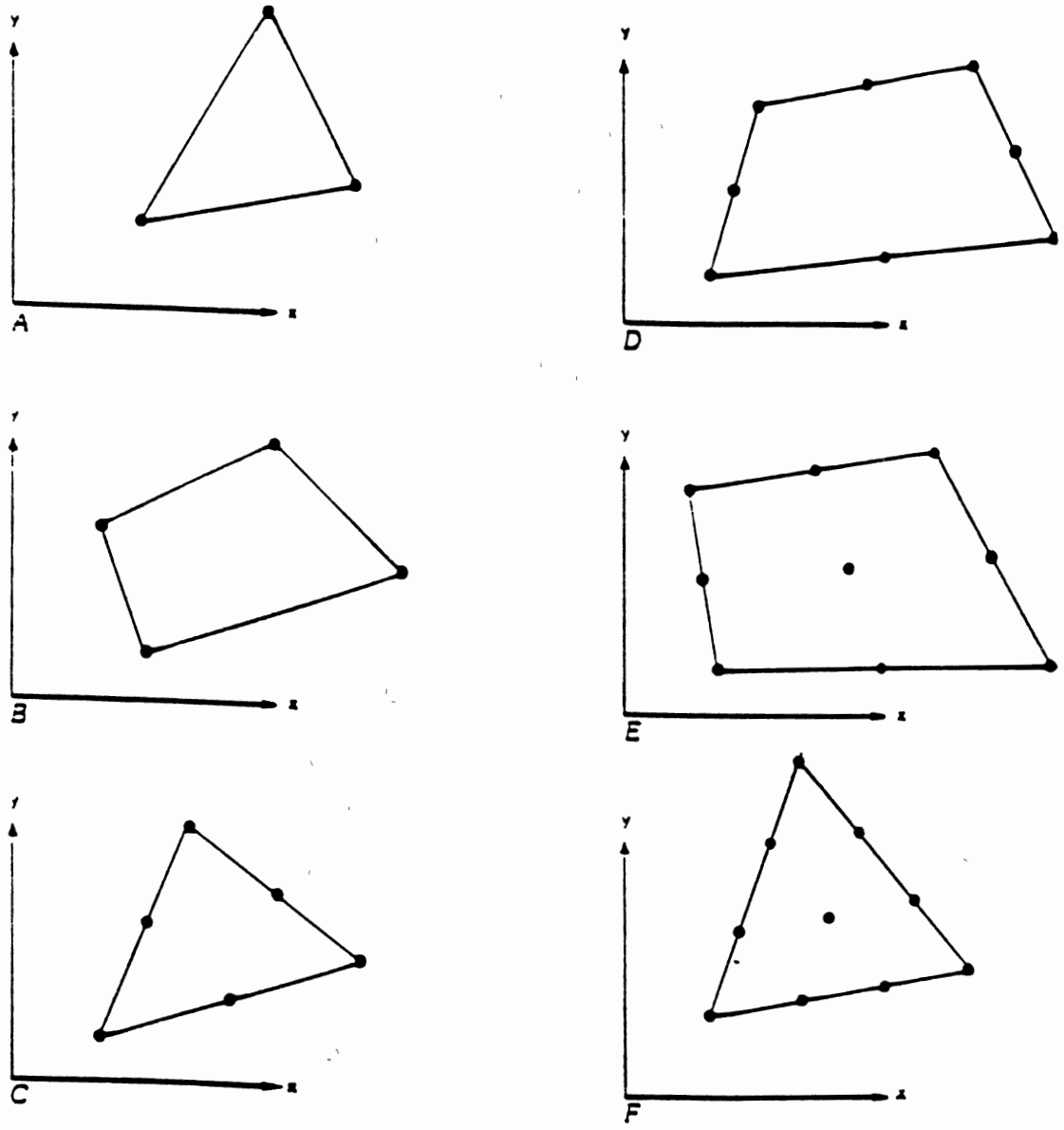

Figure 1. Examples of Two-Dimensional Elements; a) Three-Node Triangle; b) Four-Node Quadrilateral; c) Six-Node Triangles; d) Eight-Node Quadrilateral; e) Nine-Node Quadrilateral; f) Ten-Node Triangle.

CHAPTER III

FINITE-ELEMENT METHOD VERSUS FINITE-DIFFERENCE METHOD

Advantages

In the study of surface-water flow, variations in water-surface elevation and flow distribution frequently require analysis in both horizontal spatial dimensions. One dimensional models such as HY-4, HEC-2, WSPRO etc, do not have the ability to consider flow regimes that are not oriented more or less parallel to the axis of the channel. Thus they cannot follow a complicated shoreline, flow around an island, flow around piers, abutments, and other natural or man-made obstructions.

The finite-element method, which has been applied to fluid-flow problems only during the past 20 years, is ideally suited to modeling two dimensional flow over complex topography with spatially variable resistance. A two-dimensional finite-element surface-water flow model with depth and vertically averaged velocity components as dependent variables allows the user great flexibility in defining geometric features such as boundaries of water body, channels, islands, dikes and embankments. The modeler is able to use a time network in regions where geometric or

flow gradients are large and coarse network in regions where geometry and flow are more nearly uniform. The use of a two-dimensional finite-element surface-water flow model eliminates the need to use empirical coefficients other than bottom-resistance coefficients in simulating subcritical flow through constrictions. In addition, the introduction of boundary conditions is easily handled in the finite-element approach.

Basic Concepts

Alternative approaches to modeling surface-water flow in two horizontal dimensions have been developed using finite difference approaches. Price and others (1968), show that the finite-element method, requires fewer nodes (see fig. III-1) and less computational time than the finite difference method to achieve comparable accuracy in solving the one-dimensional convection-diffusion equation with a trapezoidal-rule scheme. Thacker (1978a, p.679), shows that finite-element solutions are more accurate than finite-difference solutions in solving the equations of one-dimensional gravity-wave motion where both the depth and the grid are variable.

However, any advantage that the finite-element method has in computational time is usually lost in going from three-dimensional problems because matrices generated by the finite-element method become relatively more complex than those generated by the finite-difference method as the number of dimensions increases (Thacker, 1978b). In

particular, finite-element matrices for two- and three-dimensional problems have larger band widths and are less sparse than finite-difference matrices for the same problems. Moreover, the standard finite-element approach applied to time-dependent problems gives an ordinary differential-equation system coupled in the derivatives, and requires the solution of large systems of algebraic equations at each time step, even for explicit time-integration scheme, the maximum allowable step size is smaller that for the corresponding finite-difference scheme (Cullen, 1973, p.18; Lynch, 1978, p.3-10, 3-16, 3-17; Thacker, 1978a, p.667, 678; Baker and Soliman, 1979, p.311, 312.)

In general, the finite-element method is much better adapted than the finite-difference method to modeling flow over variable terrain. A finite-element network can provide a much more realistic representation of topography and surface cover for a given number of nodes, than a finite-difference network can.

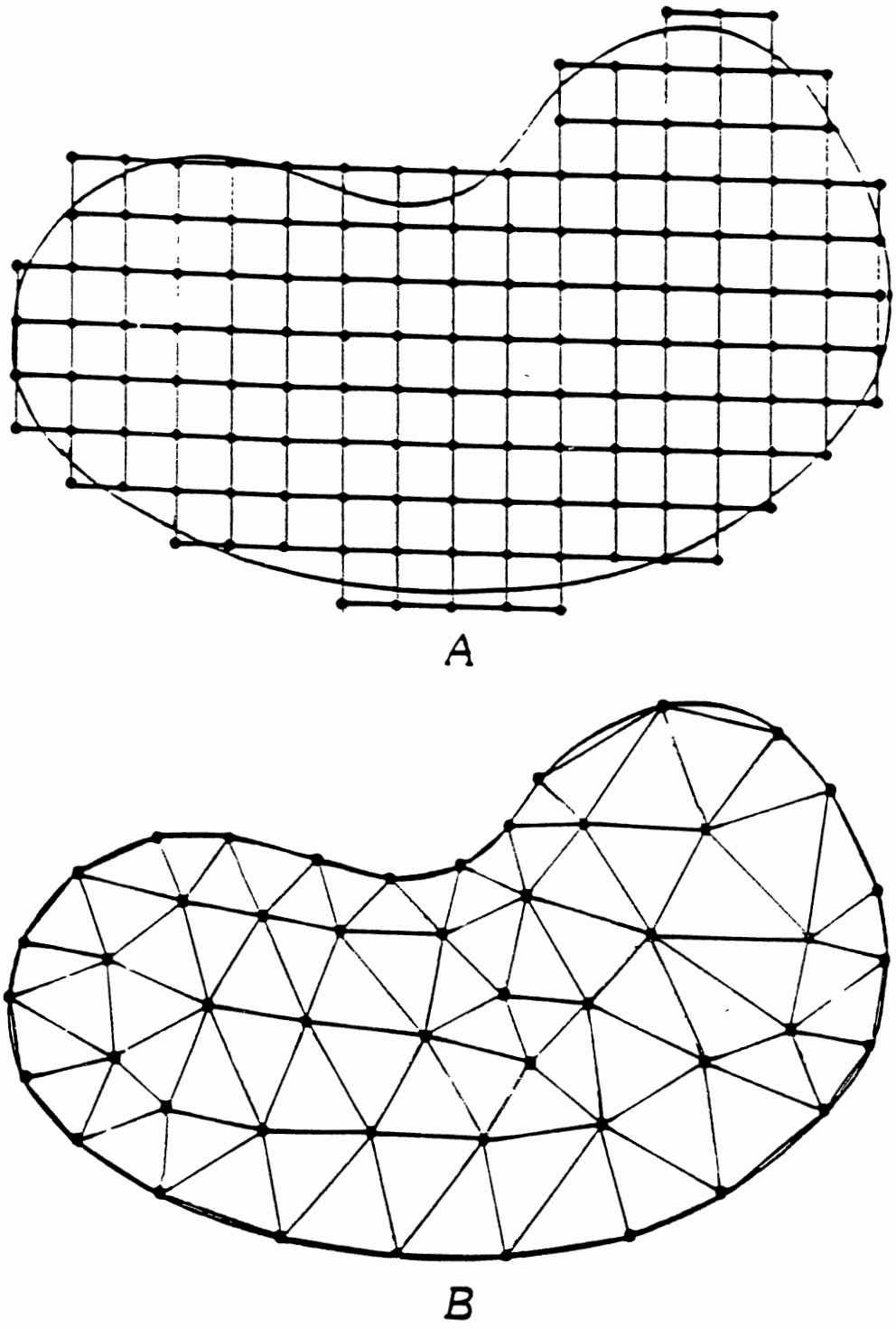

Figure 2. Finite-Difference and Finite-Element Discretizations: a) Typical Finite-Difference Grid, and b) Typical Finite-Element Grid.

CHAPTER IV

EQUATIONS OF FLOW

In many surface-water flow problems of practical engineering concern, the three-dimensional nature of the flow is of secondary importance, particularly when the width-to-depth ratio of the water body is large. In such a case, the horizontal distribution of flow quantities may be the main interest, and two-dimensional flow applications can be used to great economic advantage. In fact, the present state-of-the-art, and lack of suitable data in most cases, do not justify more complex three-dimensional solutions to most flow problems. Shallower rivers, flood plains, estuaries, harbors, and even coastal seas are examples of surface-water bodies where flows may be essentially two-dimensional in character.

FESWMS-2DH calculates depth-averaged horizontal velocities and flow depths, and the time-derivatives of these quantities if a time-dependent flow is modeled.

The equations that govern the hydrodynamic behavior of an incompressible fluid are based on the classical concepts of conservation of mass and momentum. For many practical surface-water applications, knowledge of the full three-dimensional flow structure is not required, and it is

sufficient to use meanflow quantities in two perpendicular horizontal directions. The equations that govern depth-averaged surface water flow account for the effects of friction, wind-induced stress at the water surface, fluid stresses caused by turbulence, and the effect of the earth's rotation.

The method of weighted residuals using Galerkin weighting is applied to the governing depth-averaged flow equations to form the finite element equations. Because the system of equations is nonlinear, Newton's iterative method (Zienkiewicz, 1977, p.452) is used to obtain a solution. To apply Newton's method, at each iteration the governing equations are used to define a residual and hence are referred to as residual equations. In addition, a matrix of derivatives with respect to each dependent variable for each residual equation is required. This matrix is called the Jacobian, or tangent, matrix and each of its members is defined by a derivative expression. The finite-element formulations of the residual and derivative equations at the ith node point are presented in the following sections. Application of boundary and other "special" conditions also is described.

Flow and Residual Expressions

The depth-averaged surface-waterflow equations are derived by integrating the three-dimensional conservation of mass and momentum equations with respect to the vertical coordinate from the bed to the water surface, assuming that

vertical velocities and accelerations are negligible (Jansen and others, 1979, p.41 for a thorough derivation). The vertically-integrated momentum equations are

$$\frac{\partial}{\partial t}(HU) + \frac{\partial}{\partial x}(\beta_{uu}HUU) + \frac{\partial}{\partial y}(\beta_{uv}HUV) + gH\frac{\partial z_b}{\partial x} + \frac{1}{2}g\frac{\partial H^2}{\partial x} - \Omega HV + \frac{1}{\rho}[\tau_x^b - \tau_x^s - \frac{\partial}{\partial x}(H\tau_{xx}) - \frac{\partial}{\partial y}(H\tau_{xy})] = 0 \qquad (4\text{-}1a)$$

in the x direction, and

$$\frac{\partial}{\partial t}(HV) + \frac{\partial}{\partial x}(\beta_{vu}HVU) + \frac{\partial}{\partial y}(\beta_{vv}HVV) + gH\frac{\partial z_b}{\partial y} + \frac{1}{2}g\frac{\partial H^2}{\partial y} + \Omega HU + \frac{1}{\rho}[\tau_y^b - \tau_y^s - \frac{\partial}{\partial x}(H\tau_{yx}) - \frac{\partial}{\partial y}(H\tau_{yy})] = 0 \qquad (4\text{-}1b)$$

in the y direction, and the continuity (conservation of mass) equation is

$$\frac{\partial H}{\partial t} + \frac{\partial}{\partial x}(HU) + \frac{\partial}{\partial y}(HV) = 0 \ , \qquad (4\text{-}1c)$$

where β_{uu}, β_{uv}, β_{vu}, and β_{vv} are momentum correction coefficients that account for the variation of velocity in the vertical direction; g is gravitational acceleration; Ω is the Coriolis parameter; ρ is the density of water, which is assumed constant; τ_x^b and τ_y^b are bottom shear stresses acting in the x and y directions, respectively; τ_x^s and τ_y^s are surface shear stresses acting in the x and y directions, respectively; and τ_{xx}, τ_{xy}, τ_{yx}, τ_{yy} are shear stresses caused by turbulence where, for example, τ_{xy} is the shear stress acting in the x direction on a plane that is perpendicular to the y direction.

Finite element formulations for the residuals of the depth-averaged flow equation written at node i are

$$f_{1i} = \sum_e \int_{A_e} \{N_i [H\frac{\partial U}{\partial t} + U\frac{\partial H}{\partial t} + gH\frac{\partial z_b}{\partial x} - \Omega HV + \frac{1}{\rho}(\tau_x^b - \tau_x^s)]$$

$$+ \frac{\partial N_i}{\partial x}[-\beta HUU - \frac{1}{2}gH^2 + \hat{\nu}H(\frac{\partial U}{\partial x} + \frac{\partial U}{\partial x})] + \frac{\partial N_i}{\partial y}[-\beta HUV + \hat{\nu}H(\frac{\partial U}{\partial y} + \frac{\partial V}{\partial x})]\} \, dA_e$$

$$+ \sum_e \int_{S_e} N_i[(\beta HUU + \frac{1}{2}gH^2)\ell_x + \beta HUV\ell_y] \, dS_e$$

$$- \sum_e \int_{S_e} N_i[\hat{\nu}H(\frac{\partial U}{\partial x} + \frac{\partial U}{\partial x})\ell_x + \hat{\nu}H(\frac{\partial U}{\partial y} + \frac{\partial V}{\partial x})\ell_y] \, dS_e \qquad (4\text{-}2a)$$

for the momentum equation in the x-direction, and

$$f_{2i} = \sum_e \int_{A_e} \{N_i [H\frac{\partial V}{\partial t} + V\frac{\partial H}{\partial t} + gH\frac{\partial z_b}{\partial y} + \Omega HU + \frac{1}{\rho}(\tau_y^b - \tau_y^s)]$$

$$+ \frac{\partial N_i}{\partial x}[-\beta HUV + \hat{\nu}H(\frac{\partial U}{\partial y} + \frac{\partial V}{\partial x})] + \frac{\partial N_i}{\partial y}[-\beta HVV - \frac{1}{2}gH^2 + \hat{\nu}H(\frac{\partial V}{\partial y} + \frac{\partial V}{\partial y})]\} \, dA_e$$

$$+ \sum_e \int_{S_e} N_i[\beta HUV\ell_x + (\beta HVV + \frac{1}{2}gH^2)\ell_y] \, dS_e$$

$$- \sum_e \int_{S_e} N_i[\hat{\nu}H(\frac{\partial U}{\partial y} + \frac{\partial V}{\partial x})\ell_x + \hat{\nu}H(\frac{\partial V}{\partial y} + \frac{\partial V}{\partial y})\ell_y] \, dS_e \qquad (4\text{-}2b)$$

for the momentum equation in the y-direction, and

$$f_{3i} = \sum_e \int_{A_e} M_i[\frac{\partial H}{\partial t} + H\frac{\partial U}{\partial x} + U\frac{\partial H}{\partial x} + H\frac{\partial V}{\partial y} + V\frac{\partial H}{\partial y}] \, dA_e \qquad (4\text{-}3)$$

for the continuity equation where Σ_e indicates the summation over all elements, A_e indicates an element surface, S_e indicates an element boundary, and l_x and l_y are the direction cosines between the outward normal to the boundary and the x and y directions, respectively. All second-derivative terms in the momentum equation have been integrated by parts using Green's theorem. Reduction of the

order of the expressions in this way allows use of quadratic functions to interpolate velocities. The convective and pressure terms also have been integrated by parts. Integration by parts of the convective terms simplifies the finite element equation formulation, and integration by parts of boundary conditions. The last boundary integral in the two momentum residual expressions represents the lateral stress resulting from the transport of momentum by turbulence.

Time Expressions

Expressions 4-1, 4-2, and 4-3 apply to a particular instant in time. If a steady-state solution is desired, all the time derivatives are equal to zero and do not need to be evaluated. However if the solution is time dependent, the residuals need to be integrated with respect to time as well as with to space. Time integration is accomplished using an implicit finite difference representation of the time derivatives. For example, the derivative of U with respect to time at the end of a time step is computed as

$$\frac{\partial U}{\partial t} = \frac{1}{\theta \Delta t}(U - U_o) - \frac{(1 - \theta)}{\theta}\left(\frac{\partial U}{\partial t}\right)_o , \qquad (4\text{-}4)$$

where 0 is a weighting coefficient ranging between 0.5 and 1; Δt is the length of the time step; and the subscript o indicates known values at the start of the time step. A simple implicit (backward Euler) time-integration scheme

results from the setting θ equal to 1, and a trapezoidal time-integration scheme results from setting θ equal to 0.5. Setting θ equal to 0.67 has been found to produce a stable solution even for relatively large time steps and also to provide a stable solution even for relatively large time steps and also to provide an accurate solution (King and Norton, 1987). The expressions for $\delta U/\delta t$ can be rearranged as

$$\frac{\partial U}{\partial t} = \alpha U - \beta_1 \ , \qquad (4\text{-}5)$$

where

$$\alpha = \frac{1}{\theta \Delta t} \ ; \qquad (4\text{-}6)$$

and

$$\beta_1 = \alpha U_o + \frac{(1 - \theta)}{\theta}\left(\frac{\partial U}{\partial t}\right)_o \ . \qquad (4\text{-}7)$$

The term β_1 contains only quantities that are known at the start of a time step.

In a similar manner, time derivatives of V and H are defined as

$$\frac{\partial V}{\partial t} = \alpha V - \beta_2 \ , \qquad (4\text{-}8)$$

and

$$\frac{\partial H}{\partial t} = \alpha H - \beta_3 \ , \qquad (4\text{-}9)$$

where

$$\beta_2 = \alpha V_o + \frac{(1 - \theta)}{\theta}\left(\frac{\partial V}{\partial t}\right)_o \ ; \qquad (4\text{-}10)$$

and

$$\beta_3 = \alpha H_o + \frac{(1 - \theta)}{\theta}\left(\frac{\partial H}{\partial t}\right)_o . \qquad (4\text{-}11)$$

Derivative Expressions

The finite element formulations of the derivatives of the depth-averaged flow equation residual are written for node i with respect to node variables at node j. The derivative expressions for the residual of the conservation of momentum equation in the x direction are:

$$\frac{\partial f_{1i}}{\partial U_j} = \sum_e \int_{A_e} \{N_i N_j [\alpha H + \frac{\partial H}{\partial t} + \frac{1}{\rho}\tau_x^b \frac{(2U^2 + V^2)}{U(U^2 + V^2)}]$$

$$+ \frac{\partial N_i}{\partial x} N_j [-2\beta HU] + \frac{\partial N_i}{\partial x}\frac{\partial N_j}{\partial x}[2\hat{\nu}H] + \frac{\partial N_i}{\partial y} N_j [-\beta HV] + \frac{\partial N_i}{\partial y}\frac{\partial N_j}{\partial y}[\hat{\nu}H]\} \, dA_e$$

$$+ \sum_e \int_{S_e} N_i N_j [2\beta HU\ell_x + \beta HV\ell_y] \, dS_e$$

$$- \sum_e \int_{S_e} \{N_i \frac{\partial N_j}{\partial x}[2\hat{\nu}H\ell_x] + N_i \frac{\partial N_j}{\partial y}[\hat{\nu}H\ell_y] \, dS_e \; ; \qquad (4\text{-}12)$$

$$\frac{\partial f_{1i}}{\partial V_j} = \sum_e \int_{A_e} \{N_i N_j [-\Omega H + \frac{1}{\rho}\tau_x^b \frac{V}{(U^2 + V^2)}]$$

$$+ \frac{\partial N_i}{\partial y} N_j [-\beta HU] + \frac{\partial N_i}{\partial y}\frac{\partial N_j}{\partial x}[\hat{\nu}H]\} \, dA_e$$

$$+ \sum_e \int_{S_e} N_i N_j [\beta HU\ell_y] \, dS_e - \sum_e \int_{S_e} \{N_i \frac{\partial N_j}{\partial x}[\hat{\nu}H\ell_y] \, dS_e \; ; \qquad (4\text{-}13)$$

$$\frac{\partial f_{1i}}{\partial H_j} = \sum_e \int_{A_e} \{N_i M_j [\frac{\partial U}{\partial t} + \alpha U - \Omega V + g\frac{\partial z_b}{\partial x} + \frac{1}{\rho}\tau_x^b \frac{1}{c_f}\frac{\partial c_f}{\partial H}]$$

$$+ \frac{\partial N_i}{\partial x} M_j [-\beta UU - gH + \hat{\nu}(\frac{\partial U}{\partial x} + \frac{\partial U}{\partial x})] + \frac{\partial N_i}{\partial y} M_j [-\beta UV + \hat{\nu}(\frac{\partial U}{\partial y} + \frac{\partial V}{\partial x})]\} \, dA_e$$

$$+ \sum_e \int_{S_e} N_i M_j [(\beta UU + gH)\ell_x + \beta UV\ell_y] \, dS_e$$

$$- \sum_e \int_{S_e} \{N_i M_j [\hat{v}(\frac{\partial U}{\partial x} + \frac{\partial U}{\partial x})\ell_x + \hat{v}(\frac{\partial U}{\partial y} + \frac{\partial V}{\partial x})\ell_y] \, dS_e \, . \quad (4\text{-}14)$$

Derivative expressions for the residual of the conservation of momentum equation in the y direction are:

$$\frac{\partial f_{2i}}{\partial U_j} = \sum_e \int_{A_e} \{N_i N_j [\Omega H + \frac{1}{\rho}\tau_y^b \frac{U}{(U^2 + V^2)}]$$

$$+ \frac{\partial N_i}{\partial x} N_j [-\beta HV] + \frac{\partial N_i}{\partial x} \frac{\partial N_j}{\partial y} [\hat{v}H]\} \, dA_e$$

$$+ \sum_e \int_{S_e} N_i N_j [\beta HV\ell_x] \, dS_e - \sum_e \int_{S_e} \{N_i \frac{\partial N_j}{\partial y} [\hat{v}H\ell_x] \, dS_e \; ; \quad (4\text{-}15)$$

$$\frac{\partial f_{2i}}{\partial V_j} = \sum_e \int_{A_e} \{N_i N_j [\alpha H + \frac{\partial H}{\partial t} + \frac{1}{\rho}\tau_y^b \frac{(U^2 + 2V^2)}{V(U^2 + V^2)}]$$

$$+ \frac{\partial N_i}{\partial x} N_j [-\beta HU] + \frac{\partial N_i}{\partial x} \frac{\partial N_j}{\partial x} [\hat{v}H] + \frac{\partial N_i}{\partial y} N_j [-2\beta HV] + \frac{\partial N_i}{\partial y} \frac{\partial N_j}{\partial y} [2\hat{v}H]\} \, dA_e$$

$$+ \sum_e \int_{S_e} N_i N_j [\beta HU\ell_x + 2\beta HV\ell_y] \, dS_e$$

$$- \sum_e \int_{S_e} \{N_i \frac{\partial N_j}{\partial x} [\hat{v}H\ell_x] + N_i \frac{\partial N_j}{\partial y} [2\hat{v}H\ell_y] \, dS_e \; ; \quad (4\text{-}16)$$

$$\frac{\partial f_{2i}}{\partial H_j} = \sum_e \int_{A_e} \{N_i M_j [\frac{\partial V}{\partial t} + \alpha V + \Omega U + g\frac{\partial z_b}{\partial y} + \frac{1}{\rho}\tau_y^b \frac{1}{c_f} \frac{\partial c_f}{\partial H}]$$

$$+ \frac{\partial N_i}{\partial x} M_j [-\beta UV + \hat{v}(\frac{\partial U}{\partial y} + \frac{\partial V}{\partial x})] + \frac{\partial N_i}{\partial y} M_j [-\beta VV - gH + \hat{v}(\frac{\partial V}{\partial y} + \frac{\partial V}{\partial y})]\} \, dA_e$$

$$+ \sum_e \int_{S_e} N_i M_j [\beta UV\ell_x + (\beta VV + gH)\ell_y] \, dS_e$$

$$- \sum_e \int_{S_e} \{N_i M_j [\hat{v}(\frac{\partial U}{\partial y} + \frac{\partial V}{\partial x})\ell_x + \hat{v}(\frac{\partial V}{\partial y} + \frac{\partial V}{\partial y})\ell_y] \, dS_e \; ; \quad (4\text{-}17)$$

where

$$\frac{\partial c_f}{\partial H} = \begin{cases} 0, \text{ if Chézy discharge coefficients are used;} \\ \\ \dfrac{\phi g n^2}{H^{4/3}}, \text{ if Manning roughness coefficients are used;} \end{cases}$$

and $\phi = 0.151$ for U.S. Customary units, and 0.333 for S.I. units. The derivative expressions for the equation continuity residuals are:

$$\frac{\partial f_{3i}}{\partial U_j} = \sum_e \int_{A_e} \{M_i \frac{\partial N_j}{\partial x}[H] + M_i N_i [\frac{\partial H}{\partial x}]\} \, dA_e \; ; \qquad (4\text{-}18)$$

$$\frac{\partial f_{3i}}{\partial V_j} = \sum_e \int_{A_e} \{M_i \frac{\partial N_j}{\partial y}[H] + M_i N_i [\frac{\partial H}{\partial y}]\} \, dA_e \; ; \qquad (4\text{-}19)$$

$$\frac{\partial f_{3i}}{\partial H_j} = \sum_e \int_{A_e} \{M_i M_j [\alpha + \frac{\partial U}{\partial x} + \frac{\partial V}{\partial y}] + M_i \frac{\partial M_j}{\partial x}[U] + M_i \frac{\partial M_j}{\partial y}[V]\} \, dA_e \; . \qquad (4\text{-}20)$$

Application of Boundary and Special Conditions

The Galerkin finite element formulation allows complicated boundary conditions to be automatically satisfied as natural conditions of the problem. These natural boundary conditions are implicitly imposed in the problem statement and require no further treatment. Those boundary conditions that are imposed explicitly are known as forced, or essential, conditions. These boundary values are prescribed by modifying the finite element equation governing that variable. In addition, special boundary conditions imposed by one-dimensional flow at culverts and

weirs can be easily applied.

Open Boundaries

Velocities and depth can be applied as essential boundary conditions at any node point on an boundary as long as the system of equations does not become overconstrained. Velocities and depth are prescribed at node i by replacing the residual expressions by

$$f_{1i} = U_i \ , \tag{4-21}$$

$$f_{2i} = V_i \ , \tag{4-22}$$

$$f_{3i} = H_i \ , \tag{4-23}$$

and replacing the derivative expressions by

$$\frac{\partial f_{1i}}{\partial U_j} = \begin{cases} 1, & \text{if } i = j \\ 0, & \text{if } i \neq j \end{cases}; \quad \frac{\partial f_{1i}}{\partial V_j} = 0; \quad \frac{\partial f_{1i}}{\partial H_j} = 0; \quad \text{(4-24a,b,c)}$$

$$\frac{\partial f_{2i}}{\partial U_j} = 0; \quad \frac{\partial f_{2i}}{\partial V_j} = \begin{cases} 1, & \text{if } i = j \\ 0, & \text{if } i \neq j \end{cases}; \quad \frac{\partial f_{2i}}{\partial H_j} = 0; \quad \text{(4-25a,b,c)}$$

Derivative expressions for the residual of the conservation of momentum equation in the y direction are:

$$\frac{\partial f_{3i}}{\partial U_j} = 0; \quad \frac{\partial f_{3i}}{\partial V_j} = 0; \quad \frac{\partial f_{3i}}{\partial H_j} = \begin{cases} 1, & \text{if } i = j \\ 0, & \text{if } i \neq j \end{cases}; \quad \text{(4-26a,b,c)}$$

where U_1, V_2, and H_1 are the specified values. Unit flow

rates are applied at node i in a similar manner by defining the momentum equation residuals as

$$f_{1i} = U_i H_i - q_{xi} \qquad (4\text{-}27)$$

and

$$f_{2i} = V_i H_i - q_{yi} \qquad (4\text{-}27)$$

and replacing the momentum equation derivative expressions by

(4-28a,b,c)

$$\frac{\partial f_{1i}}{\partial U_j} = \begin{cases} H_i, & \text{if } i = j \\ 0, & \text{if } i \neq j \end{cases}; \quad \frac{\partial f_{1i}}{\partial V_j} = 0; \quad \frac{\partial f_{1i}}{\partial H_j} = \begin{cases} U_i, & \text{if } i = j \\ 0, & \text{if } i \neq j \end{cases};$$

and (4-29a,b,c)

$$\frac{\partial f_{2i}}{\partial U_j} = 0; \quad \frac{\partial f_{1i}}{\partial V_j} = \begin{cases} H_i, & \text{if } i = j \\ 0, & \text{if } i \neq j \end{cases}; \quad \frac{\partial f_{1i}}{\partial H_j} = \begin{cases} U_i, & \text{if } i = j \\ 0, & \text{if } i \neq j \end{cases};$$

where q_{xi} and q_{yi} are specified unit flow rate s in the x and y directions, respectively, at node i.

Depth also can be applied as a natural boundary condition by using the specified value of depth at node i, H_i, to evaluate the boundary integral terms in the momentum equation residual expression 4-1 and 4-2. Contributions from the boundary-integral terms are taken as zero when derivatives of the momentum equation residuals with respect to H_i are computed.

When water depth is specified as a natural boundary condition, global mass conservation is insured and total inflow will equal total outflow in steady-state simulations. However, water depths computed at nodes where the water-

surface elevation is applied as a inflow in steady-state simulations.

The total flow through a cross section that forms part of the open boundary of a finite element network is specified, a constant is divided among the node points on the basis of conveyance. The cross section is defined by a list of node points that form a connected series of element sides. Each element side is composed of three nodes (1, 2, and 3) where nodes 1 and 3 are corner nodes, and node 2 is a midside node. Conveyance through each element side is defined as

$$K = A \sqrt{gR/c_f} \ , \qquad (4\text{-}30)$$

where R is the hydraulic radius (area divided by the wetted perimeter) of the element side; and A is the area of the element side below the water surface. Total conveyance for the cross section is computed as the sum of the conveyance of each element side that is contained in the section.

Conveyance through each element side is distributed among the three nodes that form the side as follows:

$$K_1 = K\ (1 - \zeta)/6 \ , \qquad (4\text{-}31)$$

$$K_2 = 2K/3 \ , \qquad (4\text{-}32)$$

$$K_3 = k\ (1 + \zeta)/6 \ ; \qquad (4\text{-}33)$$

where $\zeta = 5\Delta H / 12h$; $H = H3 - H1$; $h = (H1 + H3) / 2$; H1 is the depth at node 1; and H3 is the depth at node 3. Total flow normal to the open boundary at each cross section node point is computed on the basis of the ratio of conveyance

assigned to each node to the total conveyance computed for each cross section. The velocities and depth computed at each node are required to satisfy the condition that net flow across the open boundary resulting from flow at the node, will equal the assigned portion of the total cross section flow.

Solid Boundaries

Solid boundaries define features such as natural shorelines, jetties or seawalls. For viscous fluids, the velocity at a solid boundary is zero. This is commonly referred to as a "no-slip" boundary condition. A no-slip condition can be specified by applying x and y velocities of zero as essential boundary conditions. To accurately model the flow near a boundary at which a no-slip condition has been imposed, a network composed of relatively small elements is needed. However, for practical purposes a "slip" condition usually is applied at a solid boundary whereby flow is allowed to move in a direction tangent to the boundary. Imposing a slip condition at solid boundaries reduces the total number of elements needed in a network and thus decreases the number of equations that need to be solved. Slip conditions are applied at a solid boundary node by first transforming the x and y momentum equations that are associated with the node into equations that express conservation of momentum in directions that are tangent and normal to the boundary. The conservation of momentum equation for flow in the normal direction is then

replaced by a constraint equation that requires the net flow across the solid boundary that results from flow at the node point to equal zero.

Total Flow Across a Boundary

Total flow across a boundary (normal flow) at a node point comes from several sources. Flow across an open boundary is defined as

$$Q^{o}_{i} = Q^{o}_{si} + Q_{xi} \quad , \tag{4-34}$$

where Q^{o}_{si} is the flow normal to the boundary at node i that is specified directly; and Q_{xi} is the amount of the total flow through a cross section that is assigned to node i by the procedure used for open boundaries. Flow across a solid boundary is defined as

$$Q^{s}_{i} = Q^{s}_{si} + Q_{wi} + Q_{ci} \quad , \tag{4-35}$$

where Q^{s}_{si} is the flow normal to the solid boundary at node i that is specified directly; Q_{wi} is computed flow over a weir (roadway embankment) segment at node i; and Q_{ci} is the computed flow through a culvert at node i.

Along a boundary (either open or solid) where flow normal to the boundary expressions for flow in the x and y directions first are transformed into conservation of momentum residual expressions for flows in directions that are tangent and normal to the boundary. At node point i, the transformation is given by

$$f'_{1i} = f_{1i}\cos\delta + f_{2i}\sin\delta \ , \qquad (4\text{-}36)$$

and

$$f'_{2i} = -f_{1i}\sin\delta + f_{2i}\cos\delta \ , \qquad (4\text{-}37)$$

where f'_{1i} and f'_{2i} are the transformed momentum residual expressions in the tangential and normal directions, respectively; and δ is the angle between the positive x direction and a tangent to the boundary at node i.

If flow normal to an open boundary at node i is specified, the conservation of momentum equation for flow normal to the boundary is replaced by the equation

$$a^{o}_{i}U_i + b^{o}_{i}V_i - Q^{o}_{i} = 0. \qquad (4\text{-}38)$$

If flow normal to a solid boundary at node i is specified, the conservation of momentum equation for flow normal to the boundary is replaced by the equation

$$a^{s}_{i}U_i + b^{s}_{i}V^{i} - Q^{s}_{i} = 0. \qquad (4\text{-}39)$$

The terms a^{o}_{i}, b^{o}_{i}, a^{s}_{i}, and b^{s}_{i} in expressions 4-38 and 4-39 are coefficients that are determined by requiring the computed flow across an open or solid boundary at node i to equal the specified flow, that is

$$U_i \sum_e \int_{S^o_e} N_i H\ell_x \, dS^o_e + V_i \sum_e \int_{S^o_e} N_i H\ell_y \, dS^o_e - Q^o_i = 0 \qquad (4\text{-}40)$$

and

$$U_i \sum_e \int_{S^s_e} N_i H\ell_x \, dS^s_e + V_i \sum_e \int_{S^s_e} N_i H\ell_y \, dS^s_e - Q^s_i = 0 \ , \qquad (4\text{-}41)$$

where N_i is the interpolation function for velocity at node i; S^o_e is the part of the network boundary that is open; and S^s_e is the part of the network boundary that is solid. Comparing expression 4-38 to expression 4-40, and expression 4-39 to expression 4-41, it is readily seen that

$$a_i^o = \sum_e \int_{S_e^o} N_i H \ell_x \, dS_e^o \; ; \tag{4-42}$$

$$b_i^o = \sum_e \int_{S_e^o} N_i H \ell_y \, dS_e^o \; ; \tag{4-43}$$

$$a_i^s = \sum_e \int_{S_e^s} N_i H \ell_x \, dS_e^s \; ; \tag{4-44}$$

and

$$b_i^s = \sum_e \int_{S_e^s} N_i H \ell_y \, dS_e^s \; . \tag{4-45}$$

Derivatives of the constraint equation for total flow across an open boundary are computed as

$$\frac{\partial f_{1i}}{\partial U_j} = \begin{cases} a_i^o, & \text{if } i = j \\ 0, & \text{if } i \neq j \end{cases} \; ; \tag{4-46}$$

$$\frac{\partial f_{1i}}{\partial V_j} = \begin{cases} b_i^o, & \text{if } i = j \\ 0, & \text{if } i \neq j \end{cases} \; ; \tag{4-47}$$

and

$$\frac{\partial f_{1i}}{\partial H_j} = \frac{\partial a_i^o}{\partial H_j} U_i + \frac{\partial b_i^o}{\partial H_j} V_i \; ; \tag{4-48}$$

where

$$\frac{\partial a_i^o}{\partial H_j} = \sum_e \int_{S_e^o} N_i M_j \ell_x \, dS_e^o \tag{4-49}$$

and

$$\frac{\partial b_i^o}{\partial H_j} = \sum_e \int_{S_e^o} N_i M_j \ell_y \, dS_e^o \; . \qquad (4\text{-}50)$$

$$\frac{\partial f_{2i}}{\partial U_j} = \begin{cases} a_i^s, & \text{if } i = j \\ 0, & \text{if } i \neq j \end{cases} ; \qquad (4\text{-}51)$$

$$\frac{\partial f_{2i}}{\partial V_j} = \begin{cases} b_i^s, & \text{if } i = j \\ 0, & \text{if } i \neq j \end{cases} ; \qquad (4\text{-}52)$$

Derivatives of the constraint equation for total flow across a solid boundary are computed as

$$\frac{\partial f_{1i}}{\partial H_j} = \frac{\partial a_i^s}{\partial H_j} U_i + \frac{\partial b_i^s}{\partial H_j} V_i - \frac{\partial Q_{wi}}{\partial H_j} - \frac{\partial Q_{ci}}{\partial H_j} ; \qquad (4\text{-}53)$$

where

$$\frac{\partial a_i^s}{\partial H_j} = \sum_e \int_{S_e^s} N_i M_j \ell_x \, dS_e^s ; \qquad (4\text{-}54)$$

$$\frac{\partial b_i^s}{\partial H_j} = \sum_e \int_{S_e^s} N_i M_j \ell_y \, dS_e^s ; \qquad (4\text{-}55)$$

$$\frac{\partial Q_{wi}}{\partial H_j} = \frac{3}{2} \frac{Q_{wi}}{(z_e^h - z_c)} ; \qquad (4\text{-}56)$$

and

$$\frac{\partial Q_{ci}}{\partial H_j} = \frac{1}{2} \frac{Q_{ci}}{(z_s^h - z_s^t)} \; . \qquad (4\text{-}57)$$

CHAPTER V

FIELD APPLICATION

Site Overview

The Cimarron River at the I-35 crossing is fit for a FESWMS-2DH application due to the following reasons:

1. The meandering behavior exhibited by the river,
2. The inability of the one-dimensional programs to correctly model the crossing,
3. The need for future improvement and/or control of the water flow in an effective way,
4. The need for a scour evaluation at the main structure and at the overflow structure,

The comparison of aerial photos of the site taken in 1937, 1939, 1957 & 1990 (appendix A), reveals that the Cimarron River exhibits a fair degree of meandering. Meandering behavior is part of the aging process of a stream. The behavior is not yet fully understood or explained.

The main crossing of the river at the study site is at the south side of the floodplain. Meandering is moving the main channel to the north towards the overflow structure. The main channel at this point in time, is running perpendicular to the axis of the floodplain at the

vicinity of the bridge. This aspect makes very difficult for the one-dimensional programs to model the river crossing accurately, especially at the low flows rates. In addition to this, the fact that the overflow structure has a flowline of 16.5 feet higher than the flowline of the main structure also complicates the one-dimensional approaches.

The original crossing (in use up to 1988) used an 803 foot main structure at the south side of the floodplain with a group of 4 overflow structures at 280 feet, 200 feet, 282 feet and 162 feet in length. The overflow structures were placed at increments of 900 feet, 450 feet, 400 feet, 650 feet apart. This placement discouraged concentration of flow at the higher floods on the north side of the crossing. The 1986 flood had a peak discharge of 156,000 cfs which created scour problems especially under the overflow structures. The water surface elevation reached during that flood was 898.0 feet. There is no record for the velocities. In 1988, the crossing was replaced with an 800.0 foot main structure at the south side of the crossing and a 1,360.0 foot long overflow structure at the north side of the floodplain. This design was made in an effort to lower the velocity of the water through the structures and minimize the scour damages that were previously encountered.

This arrangement though encourages a water regime, (at higher flood events) to be directed under the overflow structure and potentially move the meandering main channel towards the north side of the crossing. This move endangers farm land structures, farm land, and farming equipment

(irrigation systems, etc.) located at the vicinity and downstream of the overflow structure.

Modeling

The modeling of this site was done using the following equipment and sources of information:

a. A 3.5 foot x 3.5 foot aerial photo (scale 1:200) of the site taken from an altitude of 2900 feet on 6-13-90, (Appendix A, for reduced copy.)

b. A contour map superpositioned on the aerial photo made by G. F. M. & Associates, (not included in this report).

c. Study files and photographs taken from the ODOT's files.

d. An IBM PS-2 Model 60 Personal Computer with a math-coprocessor and a laser printer.

This information (item a, b, and c) was used to assist in the construction of an element network appropriately representing the site (fig. 4). Some of the critical aspects of the network are shape, size and placement of the elements, "n" Manning values estimation and 3-dimensional coordinate generation for the nodes.

For this application a total of 388 elements were used in a mixture of six-node triangular (fig. 5), and nine-node quadrilateral (fig. 5) elements resulting in a network with a total of 1,456 nodes (fig 4).

The element size was varied depending on the hydraulic significance of their location along with the complexity and

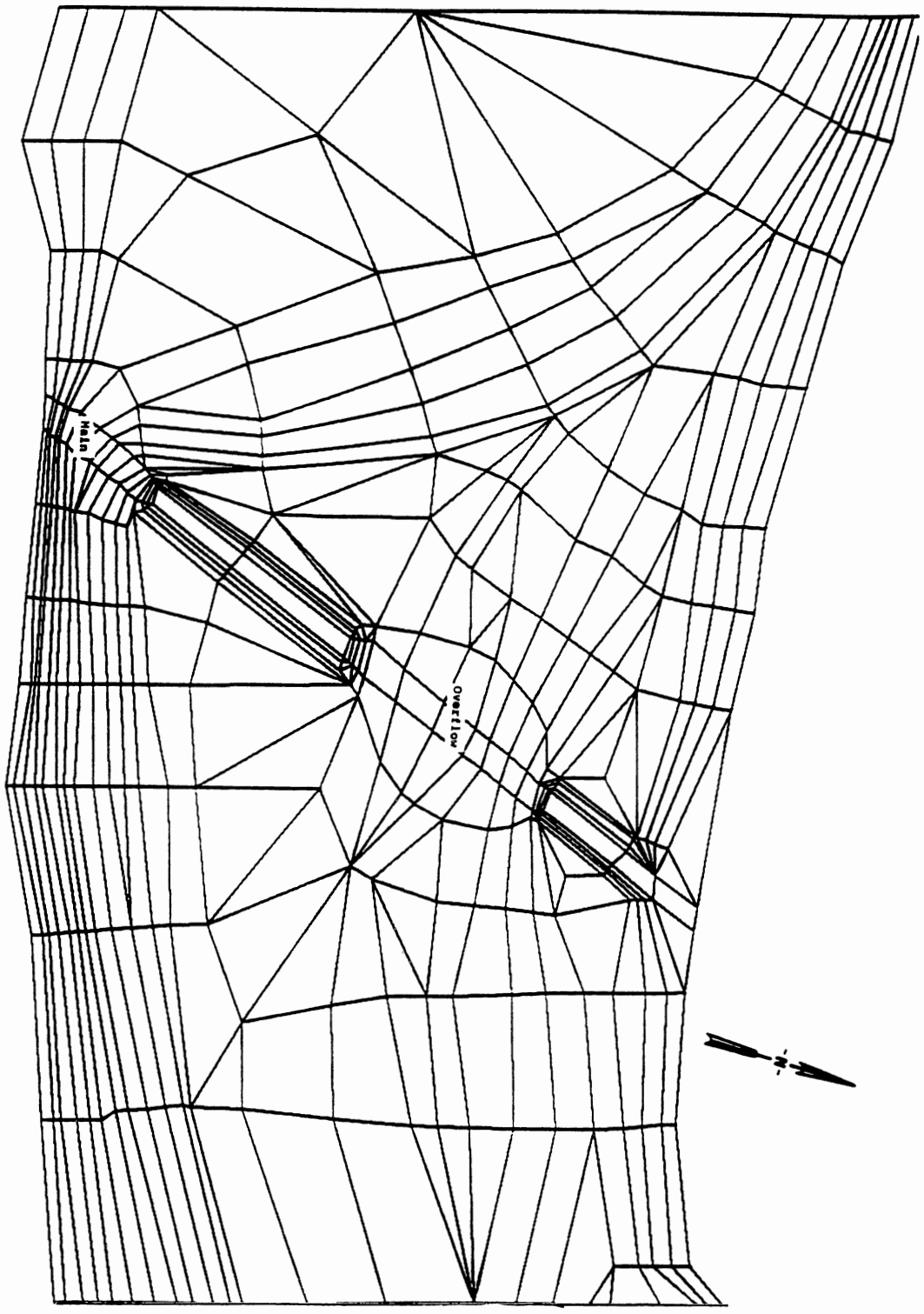

Figure 3. Site Element Network. Not to Scale

the gradient of the area. The quadrilateral elements were constructed with an aspect ratio of 3:1, but at several locations the aspect ratio was taken up to 10:1 approximately. These elements were constructed by having the longer side of the element placed along the smaller gradient, and the shortest side of it placed along the larger gradient. The node and element informations were then entered with an initial sequence in a "DINMOD" file of FESWMS-2DH version 1.0 and resequencing was performed.

The element resequencing was performed using the minimum front-growth method to obtain a direct solution of the equation that results from the application of the finite-element method. Two element assemblies were used; one at the inflow side of the element network and one at the outflow side of the network. The element assembly at the inflow side was chosen because it was given a smaller frontwidth.

Then using "FLOMOD" a steady state procedure was implemented in order to arrive at a solution. Initially a "cold start" procedure was used. During a "cold start" the water-surface elevation is assumed constant throughout the network, and the velocities are set to zero at all nodal points. Then using Q_{50} = 154,600 cfs a "hot start" was performed where the results of the cold start are used as initial conditions for the present run. The program used 2 iterations and approximately 2.0 hours to successfully complete the process (using an IBM PS-2 Model 60 Personnal Computer).

Then using "ANOMOD" the results were plotted (fig. 12) where the velocity vectors represent the depth averaged water velocity at every corner node, midside node and center node of all the "wet" elements (elements that are submerged in the water).

Another plot was made using "ANOMOD" representing the water-surface contour lines throughout the network (fig. 13) with a 0.2 foot increment.

The same procedure was used in "FLOMOD" and "ANOMOD" for the Q_{100}, and the corresponding plots (figs. 14, 15), were generated. At this time , the results of the Q_{50} run were used as the initial conditions on the Q_{100} run.

The same procedure was used for Q_{25} - Q_{10} - Q_5 runs, using the results of the Q_{50} run as initial conditions for for Q_{25}, the Q_{25} results as initial conditions for the Q_{10} run and the Q_{10} results as initial condition for the Q_5 run.

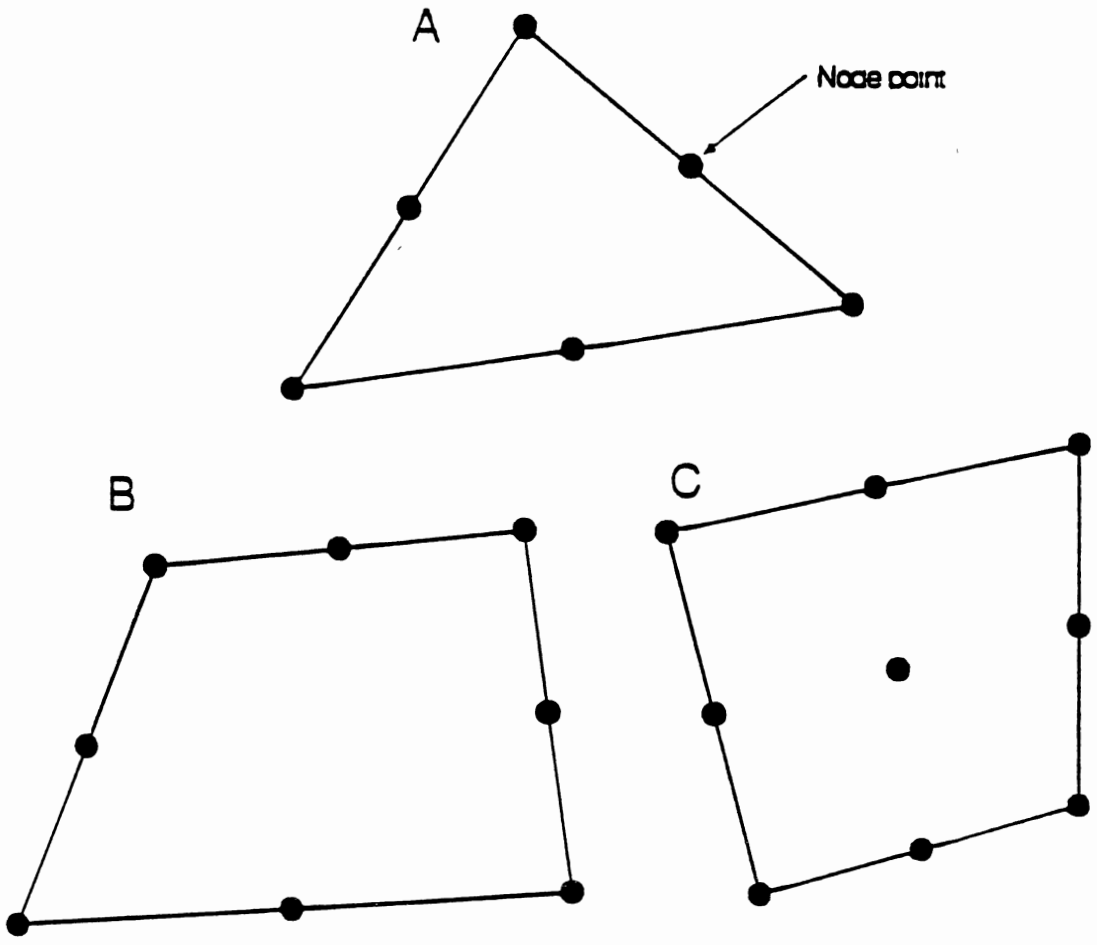

Figure 4. Examples of Two Dimensional Elements: a) Six-Node Triangle; b) Eight-Node Quadrilateral; and c) Nine-Node "Langrangian" Quadrilateral.

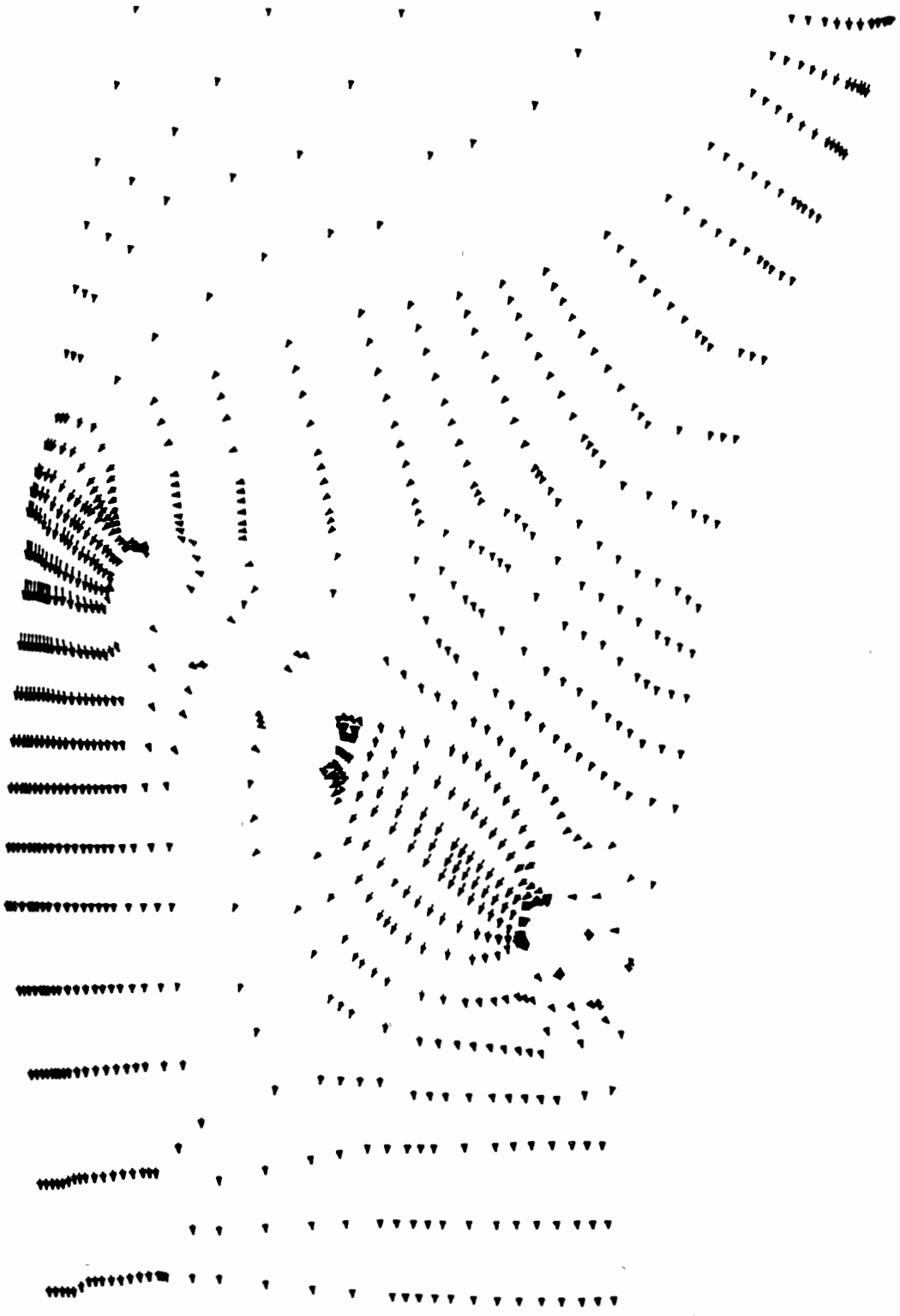

Figure 5. Velocity Vectors for Q_5 . Scale 1"=35.0 fps

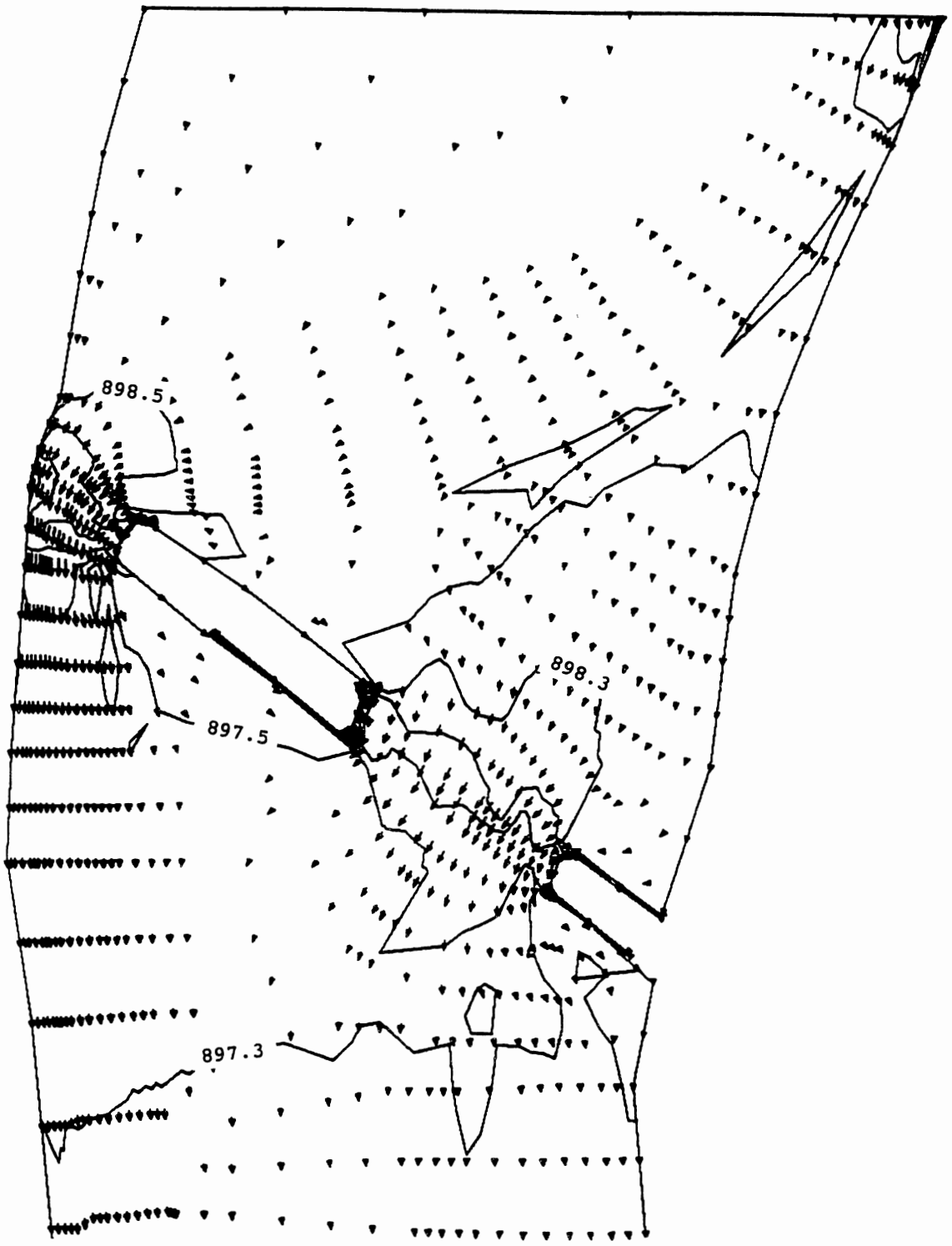

Figure 6. Water Surface Elevation for Q_s Contours.
contour increment 0.2 feet

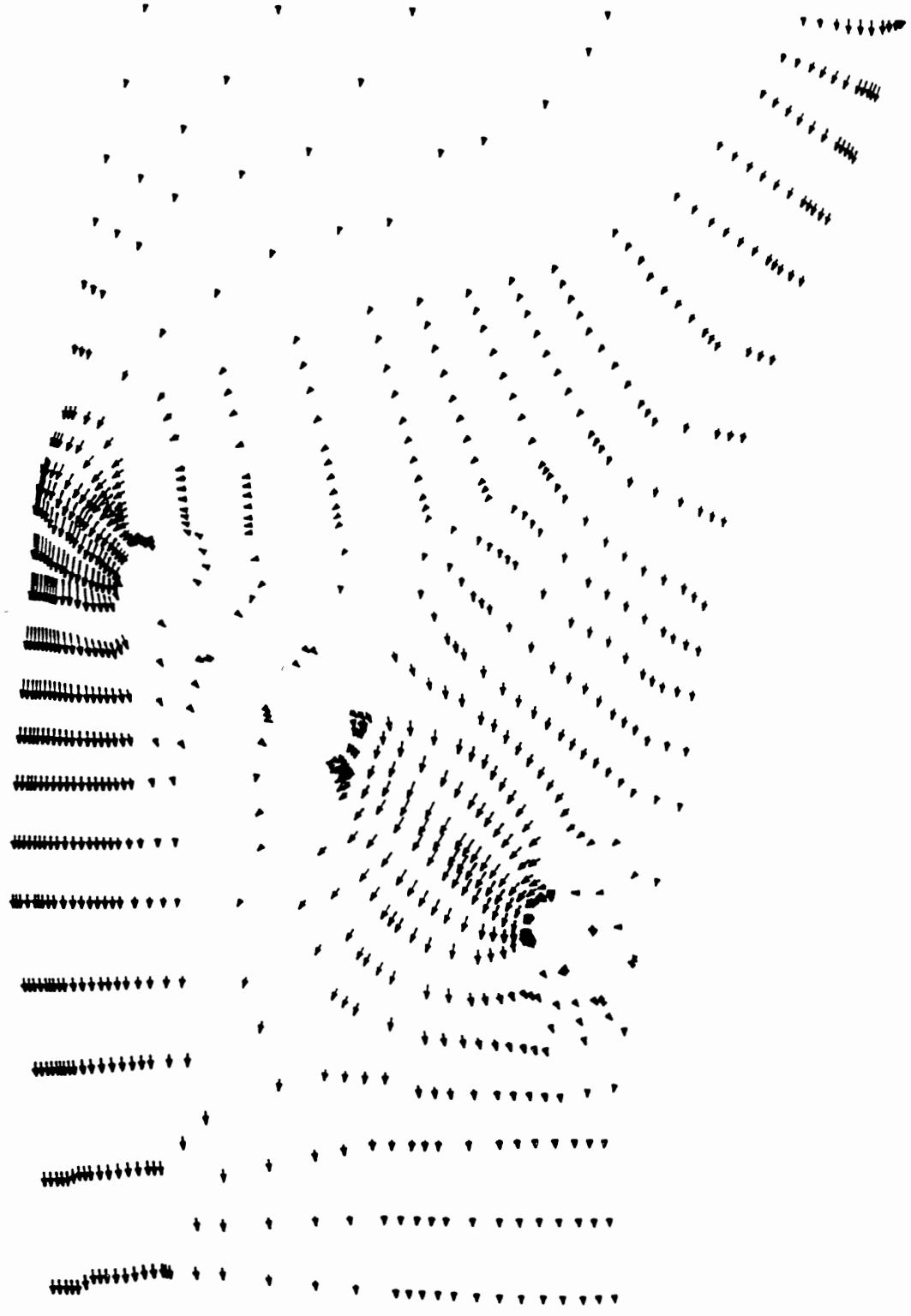

Figure 7. Velocity Vectors for Q_{10}. Scale 1"=35.0 fps

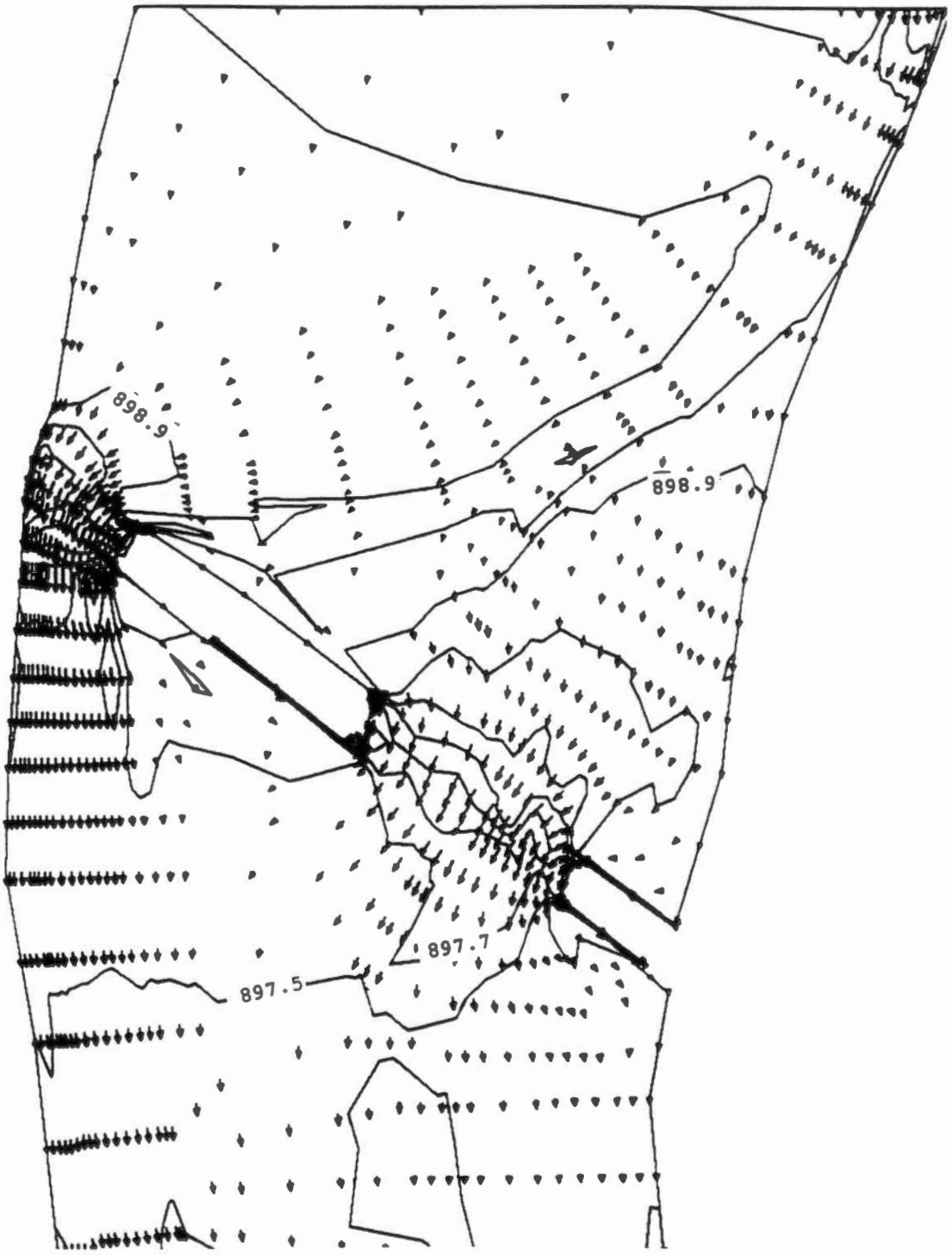

Figure 8. Water Surface Elevation for Q_{10} Contours. contour increment 0.2 feet

Figure 9. Velocity Vectors for Q_{25}. Scale 1"=35.0 fps

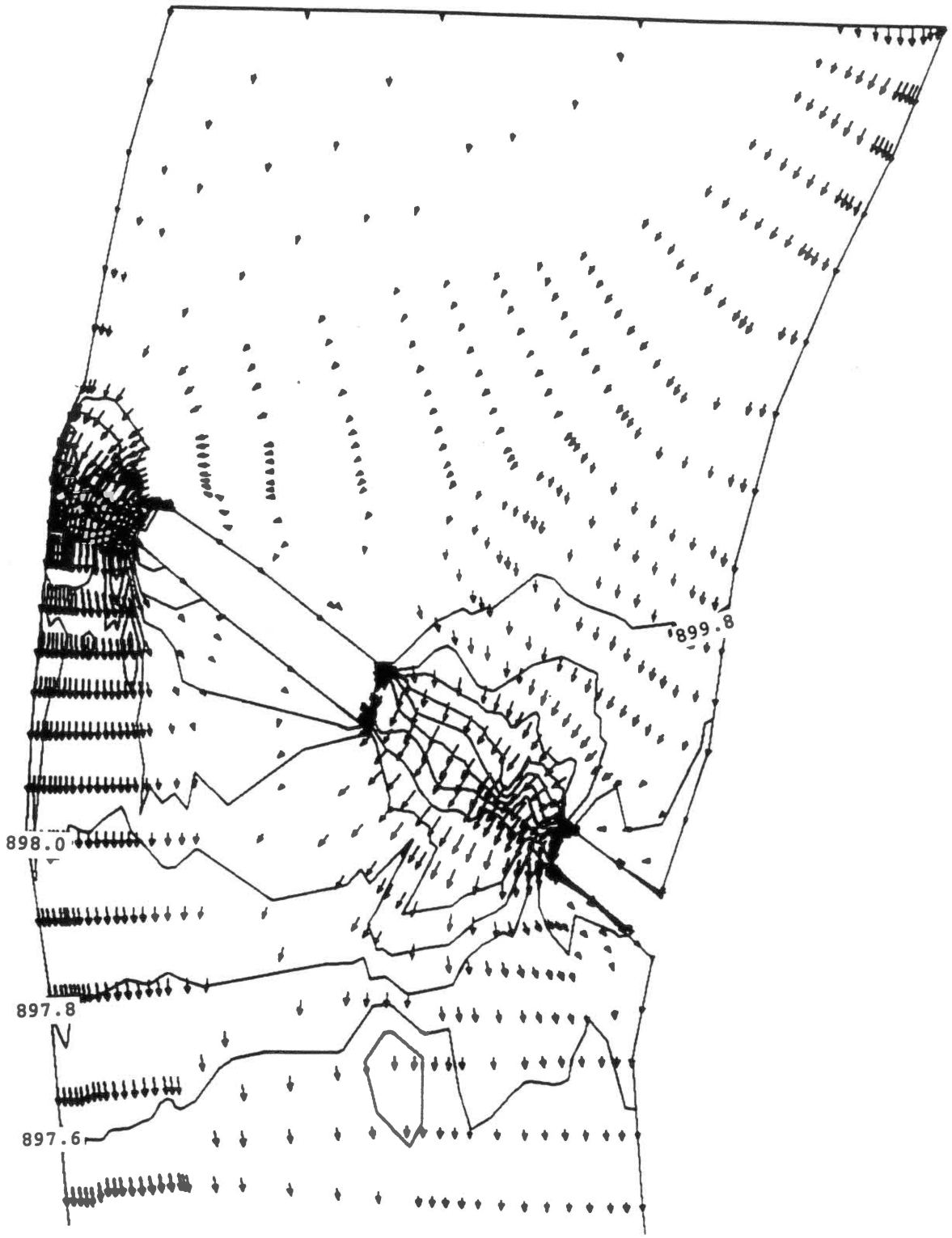

Figure 10. Water Surface Elevation for Q_{25} Contours. contour increment 0.2 feet

Figure 11. Velocity Vectors for Q_{50}. Scale 1"=35.0 fps

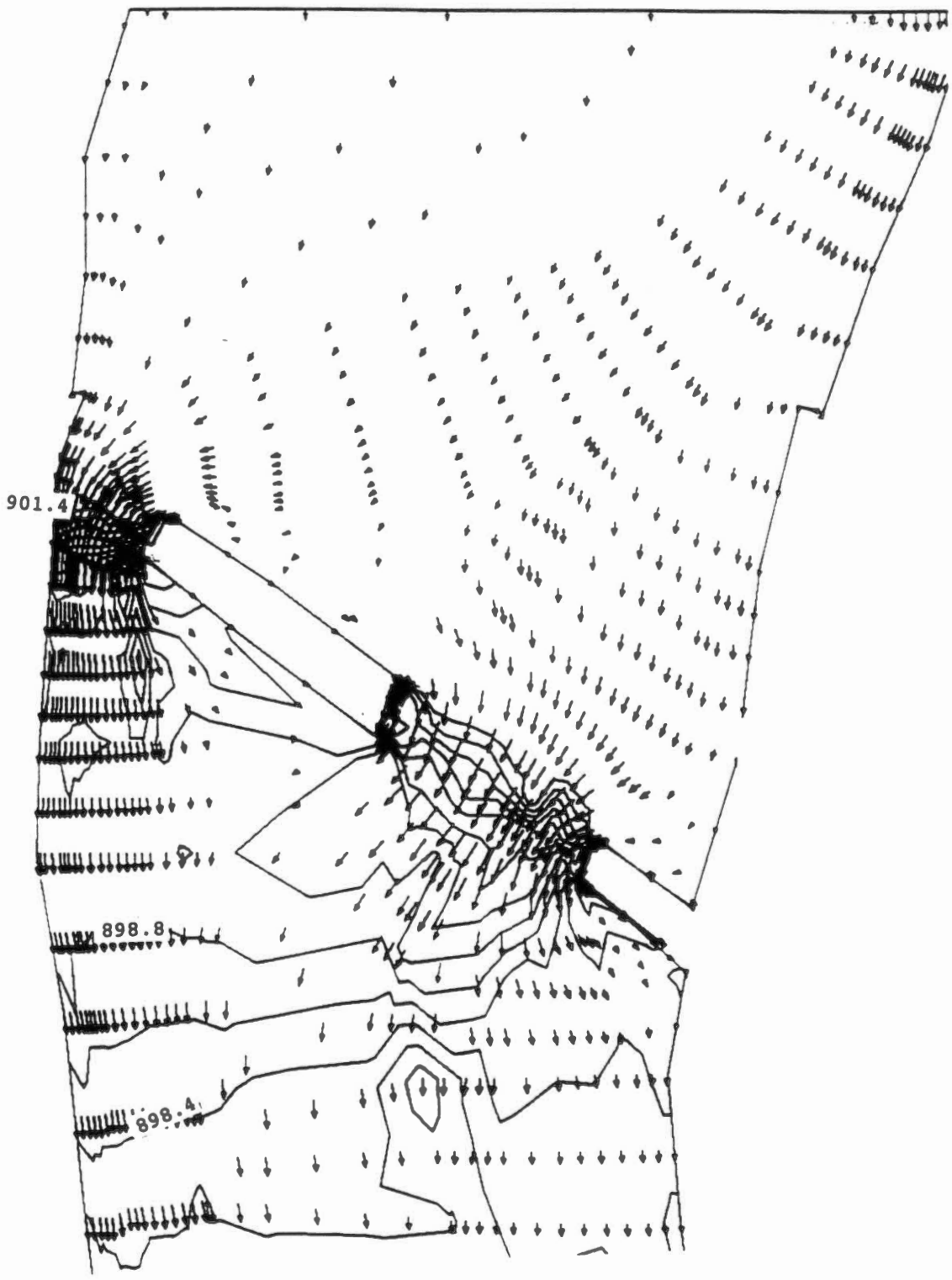

Figure 12. Water Surface Elevation for Q_{50} Contours. contour increment 0.2 feet

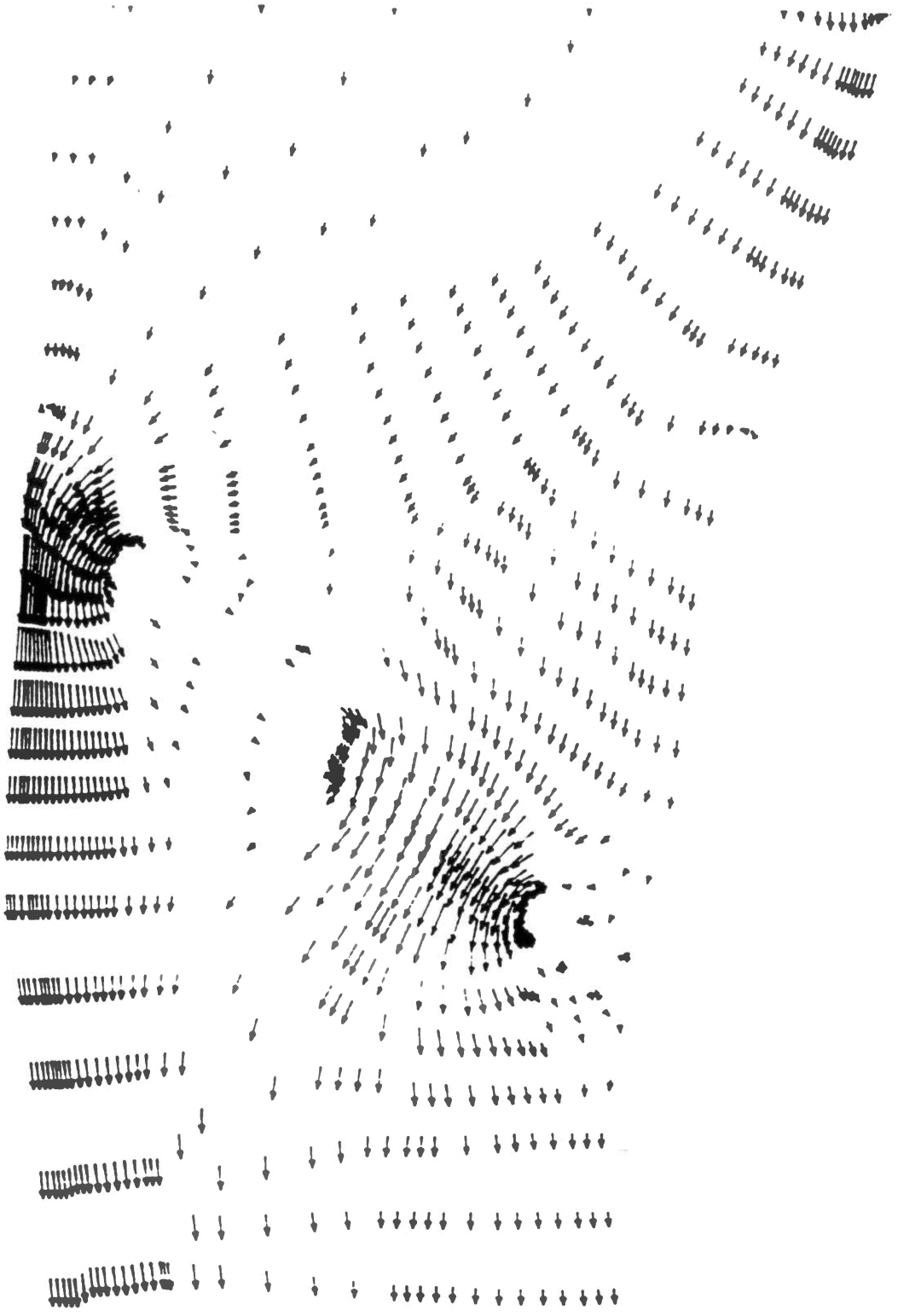

Figure 13. Velocity Vectors for Q_{100}. Scale 1"=35.0 fps

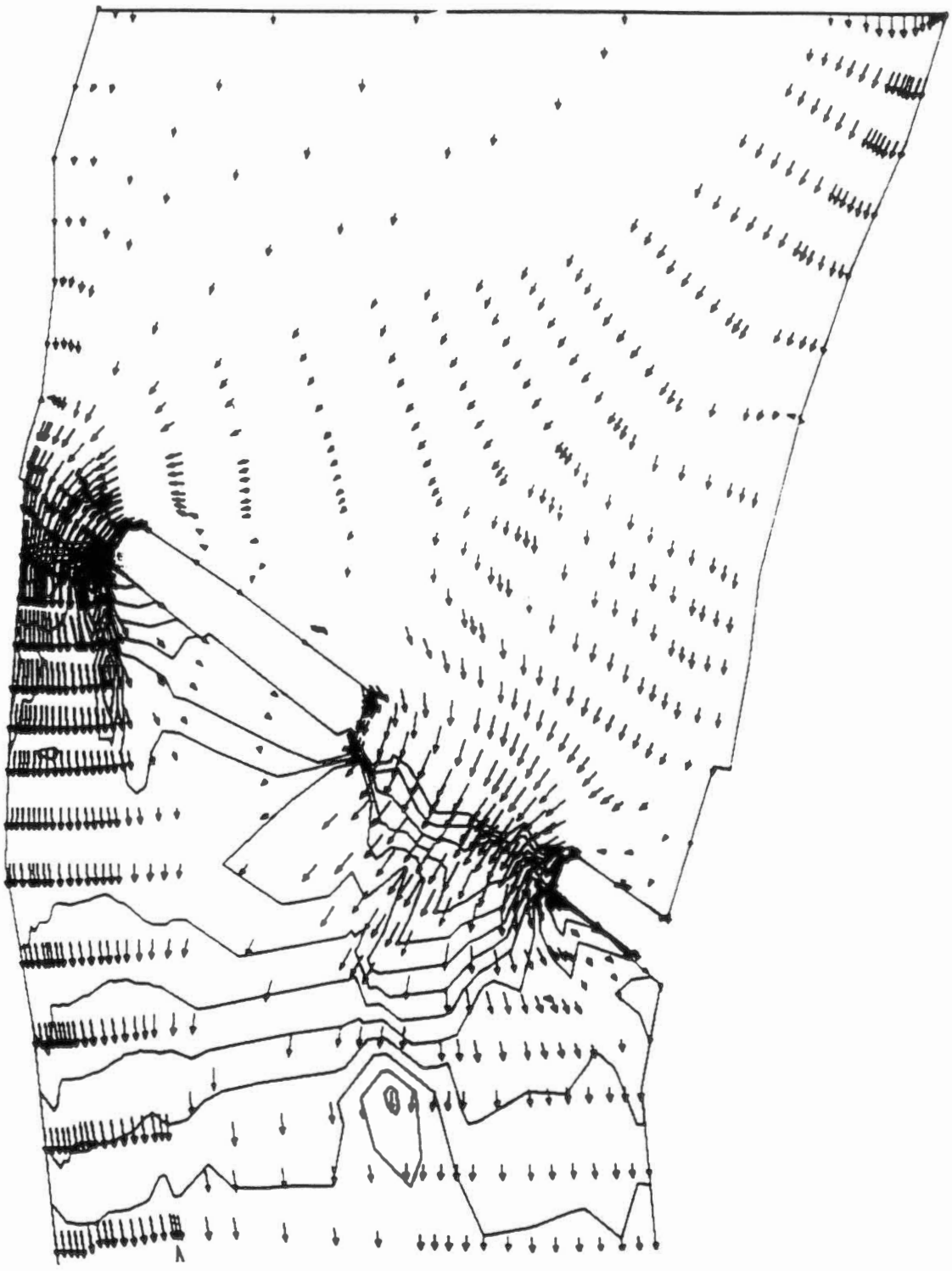

Figure 14. Water Surface Elevation for Q_{100} Contours. contour increment 0.2 feet

CHAPTER VI

RESULTS AND DISCUSSION

Comparison with HY-4 & WSPRO

The discharges utilized in this study were based on the analysis of the annual peaks from 1927 thru 1971. A new discharge-frequency curve was developed by adding annual peaks of the years 1972 thru 1986, to the existing annual peaks, and then performing a statistical analysis using Log-Pearson Type III distribution (see Appendix C). The results were as follows:

Q_5 = 63,085 cfs

Q_{10} = 88,650 cfs

Q_{25} = 125,040 cfs

Q_{50} = 154,600 cfs

Q_{100} = 185,800 cfs

Q_{500} = 264,600 cfs

These results were produced in 1987 by the Hydraulics Branch of the O.D.O.T. Bridge Division and are used for this analysis (see Appendix C).

A comparison with the 1987 WSPRO study used to design the existing bridge and overflow structure configuration and an attempt with HY-4 yielded the observations in table 6-1, 6-2 and 6-3 (Appendix B).

The comparison between the values for runoff, velocitites and water surface elevations obtained by the three programs will be focused on the results of the Q_{50} and Q_{100} events. The lower frequency events will not be closely examined and compared due to the more critical effect that the ground surface shape, slope, and cover have into the calculations. The one dimensional programs utilize a uniform cover and shape along the flow direction, but FESWMS-2DH uses the cover and slope variation needed to depict reality with the greater accuracy.

The results of the above mentioned approaches into the flow analysis is that as the waterway becomes shallower the local differences become more pronounced.

The discharge distribution (table 6.3) for Q_{50} reveals that at the main structure the results are showing a difference of 4 % between FESWMS-2DH and WSPRO and a difference of 15 % between FESWMS-2DH and HY-4. The overflow structure discharge results for Q_{50} are showing a difference of 6 % between FESWMS-2DH and WSPRO and a difference of 22 % between FESWMS-2DH and HY-4.

The main structure discharge for Q_{100} reveals a difference of 2 % between FESWMS-2DH and WSPRO and a difference of 12 % between FESWMS-2DH and HY-4. The overflow structure discharge results for Q_{100} are showing a

difference of 4 % between FESWMS-2DH and WSPRO and a difference of 18 % between FESWMS-2DH and HY-4.

The water surface elevation reported in table 6-2 for Q_{50} at the main structure show a difference of 0.1 to 2.2 feet between FESWMS-2DH and WSPRO and a difference of 1.0 to 3.1 feet between FESWMS-2DH and HY-4. The overflow structure watersurface elevations show a difference of 0.9 to 1.7 feet between FESWMS-2DH and WSPRO and a difference of 0.0 to 2.6 feet between FESWMS-2DH and HY-4. The water surface elevations for Q_{100} at the overflow structure show a difference of 0.1 to 2.4 feet between FESWMS-2DH and WSPRO and a difference of 0.8 to 1.7 feet between FESWMS-2DH and HY-4.

The reported range of the water surface elevations produced by FESMWS-2DH are depicting the superelevation that the water surface assumes under the main structure due to the almost 90° turn, and the nonuniformity of the surface cover under the overflow structure. The effect of the nonuniformity is a water surface elevation rising over the high friction values and dropping over the lower ones as it would in reality. The one dimensional programs report a uniform average water surface elevation.

The velocities reported in table 6-1 show that for Q_{50} at the main structure the difference is from 0.7 to 2.9 feet per second between FESWMS-2DH and WSPRO and 0.8 to 1.4 feet per second between FESWMS-2DH and HY-4. The overflow structure velocity distribution shows for Q_{50} the difference of 1.0 to 2.8 feet per second between FESWMS-2DH and WSPRO

and 1.2 to 2.6 feet per second between FESWMS-2DH and HY-4. The velocities reported for Q_{100} at the main structure show a difference of 0.1 to 4.6 feet per second between FESWMS-2DH and WSPRO and 1.6 to 2.9 feet per second between FESWMS-2DH and HY-4.

The overflow structure comparison reveals for Q_{100} a difference of 1.8 to 3.8 feet per second between FESWMS-2DH and WSPRO and 2.6 to 3.0 feet per second between FESWMS-2DH and HY-4.

Validity of the Results

After studying the results obtained with the implementation of FESWMS-2DH, HY-4 and WSPRO for Q_{50} and Q_{100} it can be seen that Q_{50} and Q_{100} (tables 6-1, 6-2 and 6-3) it is noted that the discharge distribution between the main and overflow structures varies from 2.0 % to 6.0 % between FESWMS-2DH and WSPRO. This is a very favorable comparison between FESWMS-2DH and HY-4 that reveals a variation of 12.0 % to 22.0 %. The comparison of the results between WSPRO and HY-4 reveals a variation of 11.0 % to 14.0 %. This variation is attributed to the fact that HY-4 is a relatively elementary program utilizing only one cross section in order to represent the site hydraulic characteristics. This variation in discharge distribution renders HY-4 invalid for this application. The same conclusion was drawn in 1987 when the existing crossing configuration was designed, and WSPRO was chosen to model the site.

The results comparison for the velocities between FESWMS-2DH and WSPRO reveal variations from 0.1 to 4.6 feet per second. This velocity variation is attributed to the fact that FESWMS-2DH reports depth averaged point velocities but WSPRO reports average flood plain velocities.

This is a favorable comparison because uniform flood plain velocities do not exist in real life. WSPRO makes this assumption on the uniformity of flow, in order to arrive at a solution.

The results comparison for the water surface elevations between FESWMS-2DH and WSPRO reveal variations from 0.1 to 2.4 feet. These variations are attributed to the superelevation that the water surface is assuming under the main bridge and the manning "n" value distribution under the overflow structure. These two important aspects of water flow are ignored by WSPRO by assuming a horizontal water surface elevation under both structures.

The results obtained by FESWMS-2DH are reasonably close to WSPRO for Q_{50} and Q_{100}. The differences encountered are attributed to

a. The different approach that the two dimensional program (FESWMS-2DH) is utilizing in order to analyze the crossing (two dimensional conservation of momentum equation versus one dimensional energy equation).

b. The nonuniformity of ground and cover characteristics that FESWMS-2DH is utilizing and

c. The depth averaged point velocities and elevation

that FESWMS-2DH is reporting versus the average velocities and water surface elevation that WSPRO is reporting.

CHAPTER VII

CONCLUSIONS AND RECOMMENDATIONS

Conclusions

1. The microcomputer applications of FESWMS-2DH can be used to evaluate the complex hydraulics of unusual river crossings such as the Cimarron River and Interstate-35. The great advantage of its use is the fact that it reports depth average point velocities, direction and point water surface elevations. This information can be used to evaluate potential scour areas, effectiveness of flow control devices and structures such as jetties, spur dikes etc.
2. This study appears to be valid and reasonable. FESWMS-2DH utilizes the discharge distribution within 2.0 % to 6.0 % of the one utilized by the WSPRO study used to design the existing crossing. The differences that are seen in the water surface elevation and velocities reported are attributed to the assumption of uniform velocity and horizontal water surface elevation that the one dimensional programs make. The only resevration comes from the lack of physical evidence -

real data observed at the site as it is today so the ultimate comparison can be carried out.

3. FESWMS-2DH is one of the most versatile tools available today, for the study of hydraulic problems due to its ability to depict unusual ground characteristics, slope variations, friction variations, etc.

Recommendations

A gage needs to be installed monitoring the runoff-stage versus velocity at the site.

The data obtained from that gage can be used to "calibrate" if need to, the FESWMS-2DH model for flow events. Then by basing the higher event runs on the results of the real events, the program will arrive at final results that can be adopted with a great degree of confidence.

BIBLIOGRAPHY

Atkinson, K.E., 1978, An Introduction to Numerical Analysis: New York, John Wiley, p.587.

Baker, A.J., and Saliman, M.O. 1979, Utility of a Finite Element Solution Algorithm for Initial-Value Problems: Journal of Computational Physics, vol. 32, no. 3, p.289-324.

Becker, E.B., Carey, G.F., and Oden, J.T., 1981, Finite Elements: An Introduction: Englewood Cliffs, N.J., Prentice Hall, p.258.

Bradley, J.N., 1978, Hydraulics of Bridge Waterways (2nd ed.): Federal Highway Administration Hydraulic Design Series, no. 1, p.111.

Bridge Waterways Analysis Model: Research Report. Shearman, J.O., Kirby, W.H., Schneider, V.R., Flippo, H.N., Sept. 1985.

Chow, V.T., 1988, Open Channel Hydraulics: Mc-Graw Hill, p.680.

Cullen, M.J.P., 1973, A Simple Finite Element Method for Meteorological Problems: Journal of the Institute of Mathematics and its Applications, vol. 11, no. 1, p.15-31.

Federal Highway Administration, Proceedings of the Bridge Scour Symposium. Two Dimensional Flow Modeling of Schoharie Creek at the Thruway Bridge, Roy E. Trent, Report No. RD-90-035, 1989, p.

Federal Highway Administration, Finite Element Surface-Water Modeling System: Two Dimensional in a Horizontal Plane; Report No. RD-88-177 David C. Froehlich, 1989, p.

Federal Highway Administration, Guide for Selecting Mannings Roughness Coefficients for Natural Channels and Floodplains; Report No. RD-84-204, April 1984, p.

HEC-2, Water-Surface Profiles; Hydrologic Engineering Center, US Army Corps of Engineers, Sept. 1990, p.180.

Jansen, P.P., van Beudegom, L., van deu Berg, J., Devries, M., and Zanen, A., Principles of River Engineering--The Non-Tidal Alluvial River, London, Pittman, 1979, p.509.

Lynch, D.R., 1978, Finite Element Solutions of the Shallow Water Equation: Princeton, N.J., Princeton University, Department of Civil Engineering, unpublished dissertion, p.349.

Nwaugazie, F.I.L. and Tyagi, A.K., 1984, Unified Streamflow Routing by Finite Elements: Journal of Hydraulic Engineering, American Society of Civil Engineers, p.1595-1611.

Streeter, V.L., Wylie, E.B. 1985, Fluid Mechanics (8th edition), Mc-Graw Hill.

Thacker, W.C., 1978a, Comparison of Finite-Element and Finite-Difference Schemes. Part I: One-Dimensional Gravity Wave Motion: Journal of Physical Oceanography, vol. 8, no. 4, p.676-679.

Thacker, W.C., 1978b, Comparison of Finite-Element and Finite-Difference Schemes. Part II: Two-Dimensional Gravity Wave Motion: Journal of Physical Oceanography, vol. 8, no. 4, p.680-689.

Tyagi, A.K. and Nwaugazie, F.I.L., 1982, Finite Element Kinematic Model for Flood Routing: Report No. R(S)22, School of Civil Engineering, Oklahoma State University, Stillwater, Oklahoma, p.75.

U.S.G.S. Circular 1009, Review of Literature on the Finite Element Solution of the Equation of Two-Dimensional Surface-Water Flow in the Horizontal Plane, Jonathon K. Lee and David C. Froehlich, 1987.

Zienkiewicz, O.C., 1977, The Finite Element Method (3rd ed.): London, Mc-Graw Hill, p.787.

APPENDIX A

PICTORIAL HISTORY OF CIMARRON RIVER

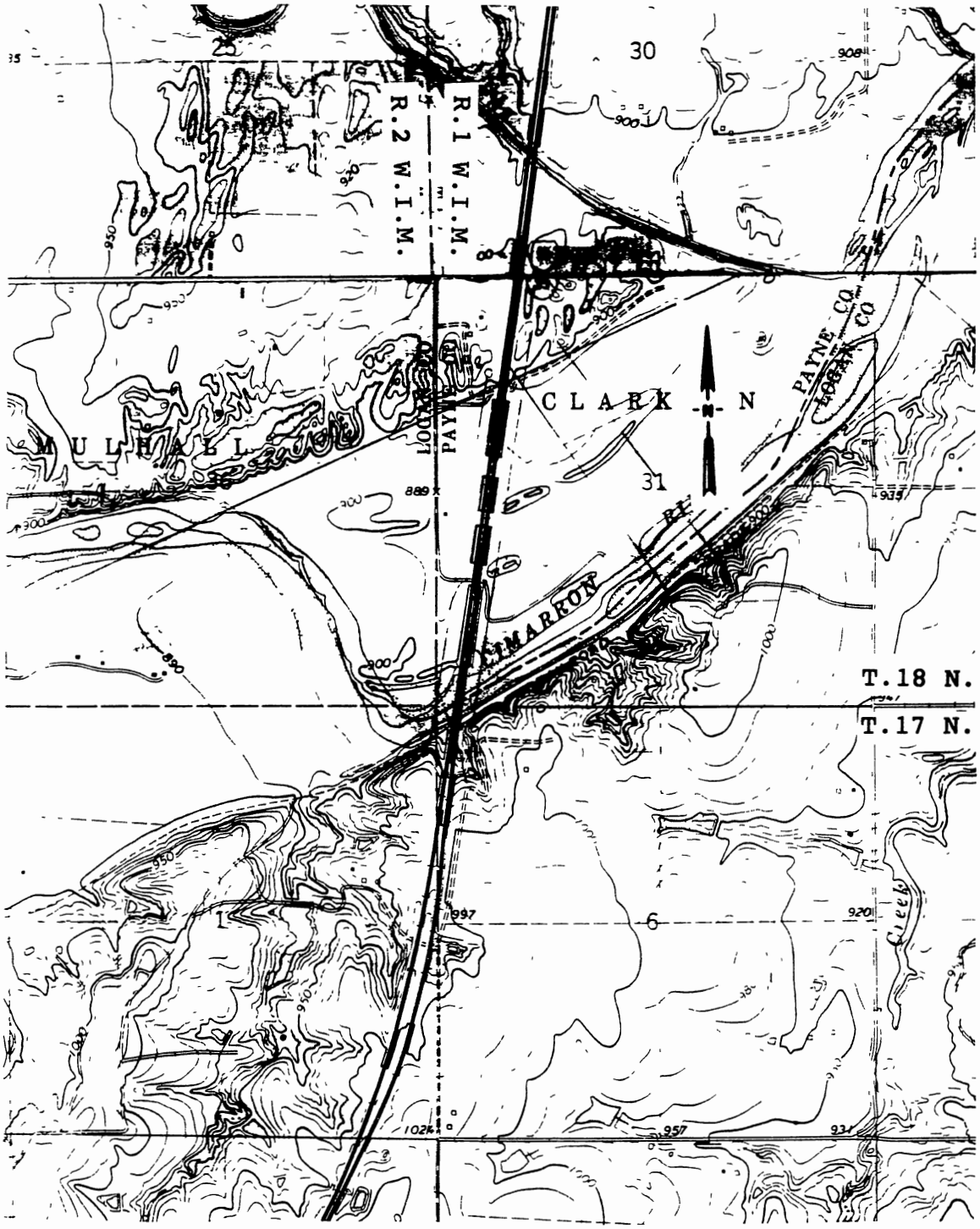

Figure 15. Location Map. Pre-1987 Conditions. Langston 7 1/2 min Quandrangle Map Photorevised 1983. Scale: 1"=2000 feet

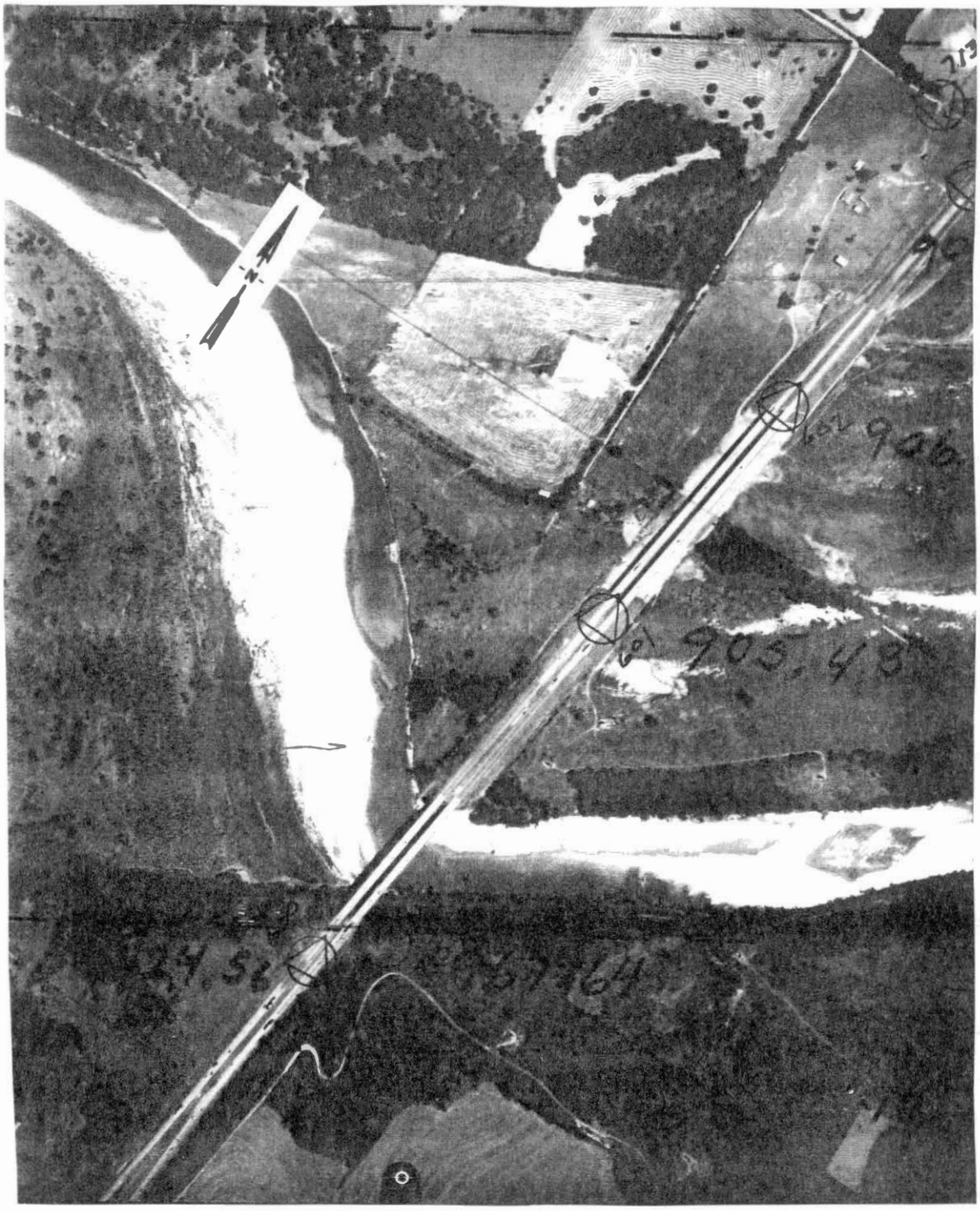

Figure 16. June 13, 1990 Conditions. Scale: 1"=1000 feet

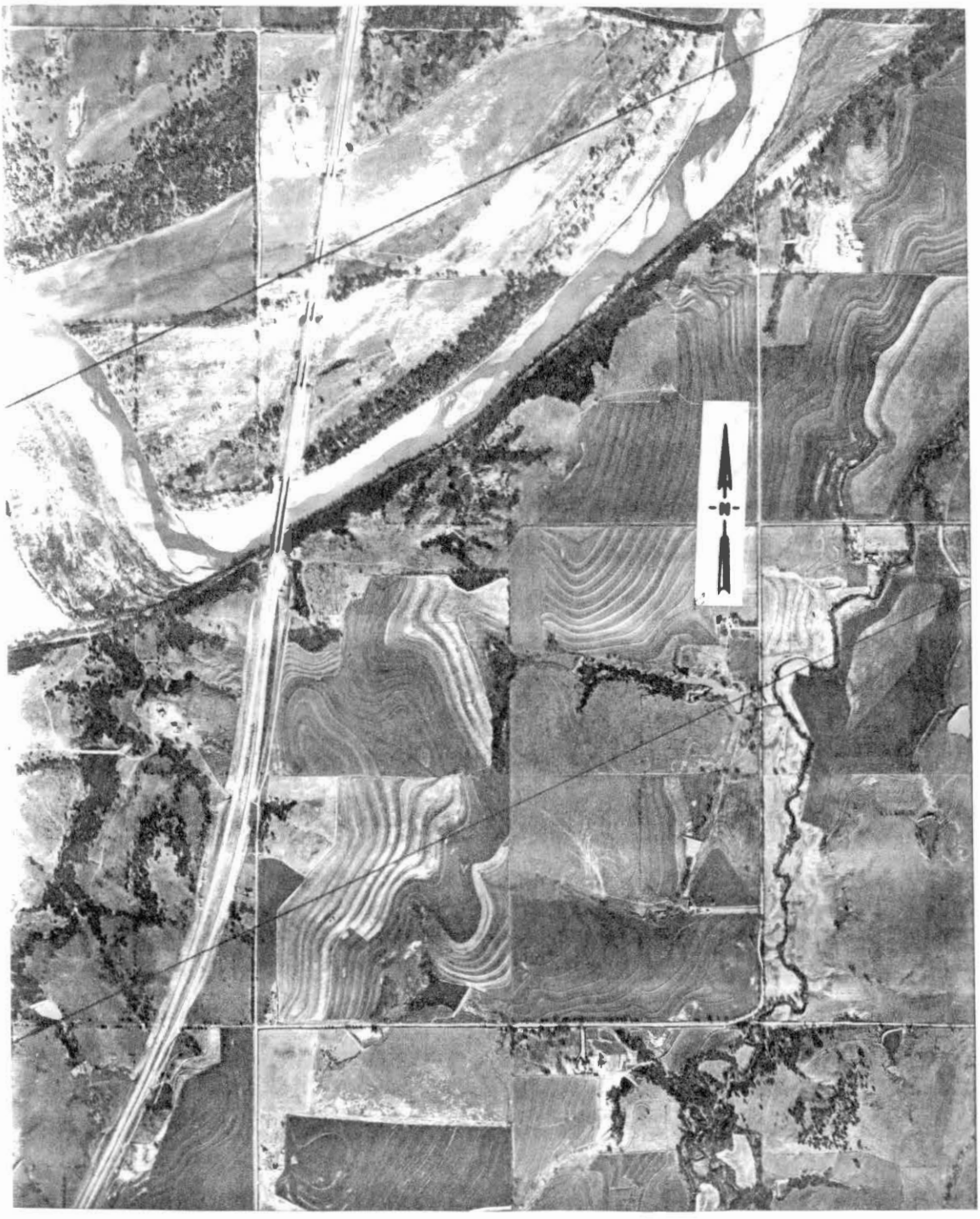

Figure 17. November 30, 1969 Conditions. Scale: 1"=2000 feet

Figure 18. July 5, 1957 Conditions. Scale: 1"=2000 feet

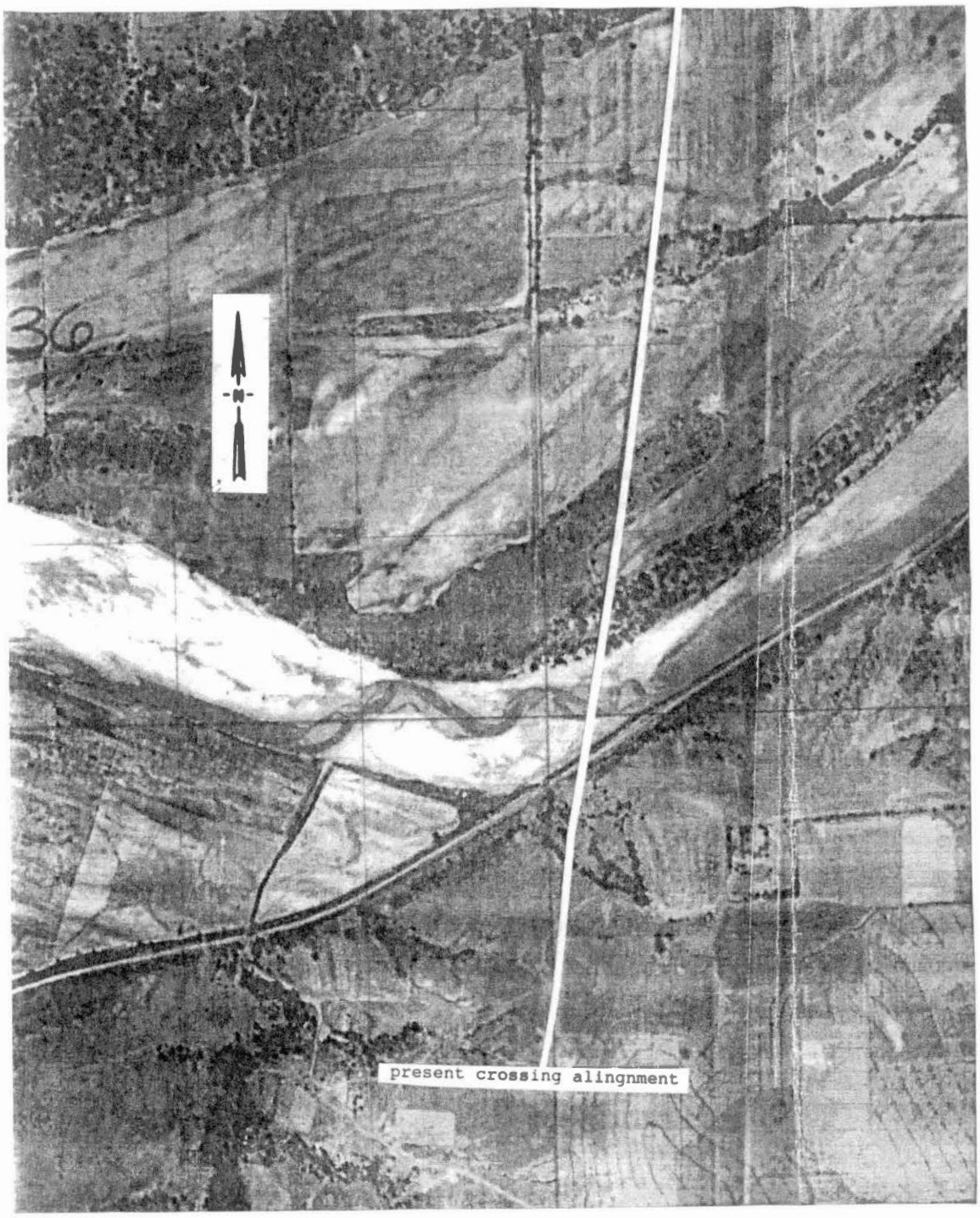

Figure 19: August 10, 1937 Conditions. Scale: 1"=2000 feet

APPENDIX B

Q_5, Q_{10}, Q_{25}, Q_{50} and Q_{100} RESULTS COMPARISON

TABLE 6-1

VELOCITIES

STRUCTURE	FREQUENCY	FESWMS	HY-4	WSPRO
Main	Q_5	(1.2 - 3.1) fps	4.9 fps	4.5 fps
Main	Q_{10}	(2.5 - 4.3) fps	5.3 fps	5.3 fps
Main	Q_{25}	(3.6 - 5.6) fps	5.4 fps	6.9 fps
Main	Q_{50}	(4.2 - 6.4) fps	5.6 fps	7.1 fps
Main	Q_{100}	(2.9 - 7.4) fps	5.8 fps	7.5 fps
Overflow	Q_5	(0.8 - 2.9) fps	2.3 fps	3.3 fps
Overflow	Q_{10}	(1.1 - 3.9) fps	2.9 fps	4.2 fps
Overflow	Q_{25}	(1.5 - 5.3) fps	3.5 fps	5.2 fps
Overflow	Q_{50}	(2.6 - 6.4) fps	3.8 fps	5.4 fps
Overflow	Q_{100}	(2.1 - 7.7) fps	4.7 fps	5.9 fps

TABLE 6-2

WATER SURFACE ELEVATIONS

STRUCTURE	FREQUENCY	FESWMS	HY-4	WSPRO
Main	Q_5	(898.1 - 898.7)	896.6	894.4
Main	Q_{10}	(898.4 - 899.4)	893.8	895.6
Main	Q_{25}	(898.9 - 900.3)	896.4	897.1
Main	Q_{50}	(899.3 - 901.4)	898.3	899.2
Main	Q_{100}	(899.7 - 901.7)	900.1	900.8
Overflow	Q_5	(897.5 - 898.3)	891.6	894.4
Overflow	Q_{10}	(897.0 - 899.5)	893.8	895.6
Overflow	Q_{25}	(898.0 - 900.1)	896.4	897.1
Overflow	Q_{50}	(898.3 - 900.9)	898.3	899.2
Overflow	Q_{100}	(898.4 - 900.9)	900.1	900.8

TABLE 6-3

DISCHARGE DISTRIBUTION

STRUCTURE	FREQUENCY	FESWMS	HY-4	WSPRO
Main	Q_5	32600 cfs	46792 cfs	36504 cfs
Main	Q_{10}	46460 cfs	59899 cfs	78884 cfs
Main	Q_{25}	64450 cfs	75605 cfs	65825 cfs
Main	Q_{50}	76440 cfs	89527 cfs	79280 cfs
Main	Q_{100}	90420 cfs	103246cfs	92020 cfs
Overflow	Q_5	30910 cfs	16923 cfs	26581 cfs
Overflow	Q_{10}	43170 cfs	29351 cfs	39766 cfs
Overflow	Q_{25}	62000 cfs	49439 cfs	59175 cfs
Overflow	Q_{50}	79680 cfs	65068 cfs	75320 cfs
Overflow	Q_{100}	97700 cfs	82550 cfs	93780 cfs

APPENDIX C

HYDROLOGY DATA

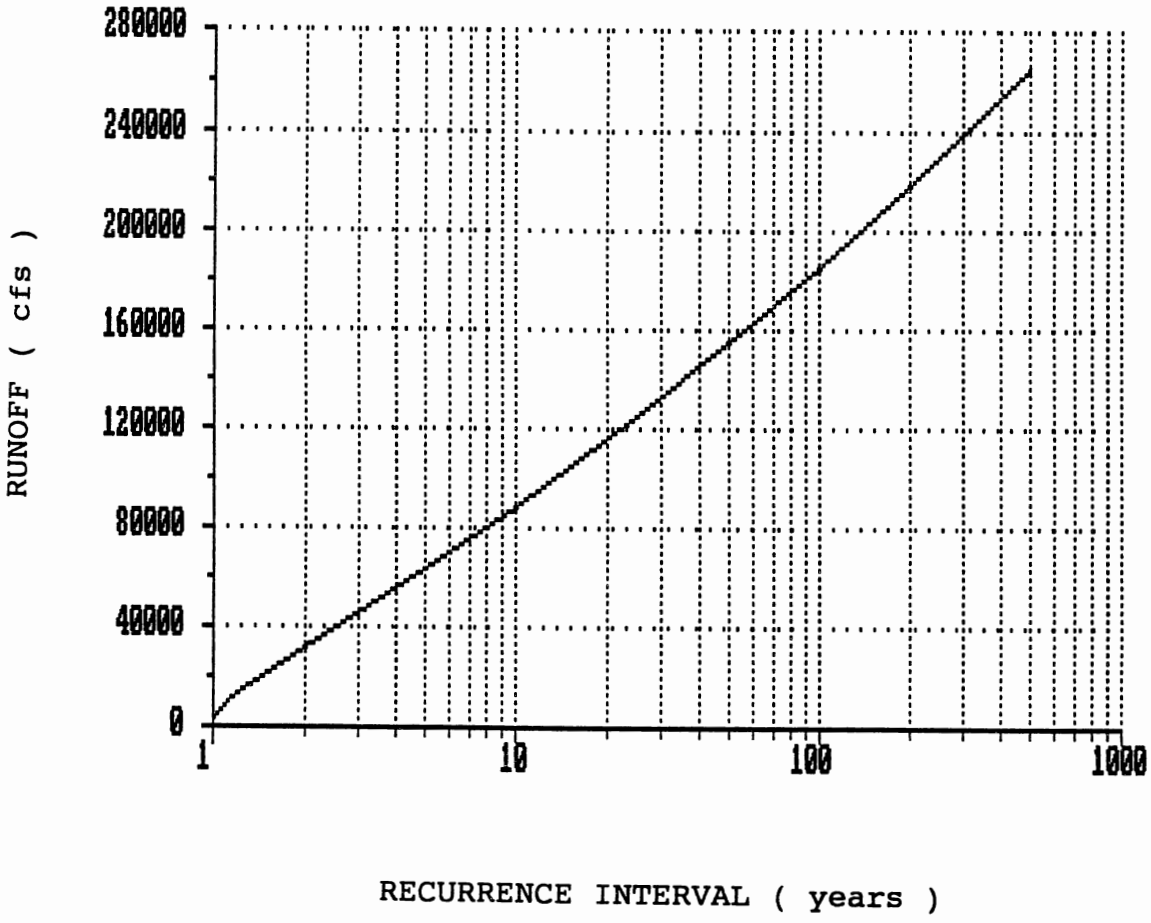

Figure 20. Runoff versus Recurrence Interval Curve

VITA

DIMITRI G. STRONGYLIS

Candidate for the Degree of

Master of Science

Thesis: WATER SURFACE PROFILES USING FESWMS-2DH MODEL

Major Field: Civil Engineering

Biographical:

Personal Data: Born on May 5, 1957, the son of Mr. and Mrs. George D. Strongylis.

Education: Graduated from The Larisa Center of Superior Technical and Professional Education in 1981, with a degree in Civil Engineering Technology. Graduated from the University of Oklahoma receiving a Bachelor of Science degree, in Civil Engineering in May, 1988; Completed the requirements for a Master of Science degree, in Civil Engineering at the Oklahoma State University in July, 1992.

Professional Experience: Engineer/Surveyor at Ross Engineering from August 1983 to September 1985; Hydraulics Engineer for the Oklahoma Department of Transportation from May 1988 to present.

Professional Organizations: Oklahoma Society of Civil Engineers - Associate Member.